

# Lightning Related Transient Luminous Events at High Altitude in the Earth's Atmosphere: Phenomenology, Mechanisms and Effects

Victor P. Pasko · Yoav Yair · Cheng-Ling Kuo

Received: 19 April 2011 / Accepted: 14 July 2011  
© Springer Science+Business Media B.V. 2011

**Abstract** This paper presents a literature survey on the recent developments related to experimental and modeling studies of transient luminous events (TLEs) in the middle atmosphere termed elves, sprites and jets that are produced in association with thunderstorm activity at tropospheric altitudes. The primary emphasis is placed on publications that appeared in refereed literature starting from year 2008 and up to the present date. The survey covers general phenomenology of TLEs and their relationships to characteristics of individual thunderstorms and lightning, physical mechanisms and modeling of TLEs, past, present and future orbital observations of TLEs, and their chemical, energetic and electric effects on local and global scales.

**Keywords** Atmospheric electricity · Lightning · Sprites · Sprite halos · Elves · Blue jets · Gigantic jets

## 1 Introduction

Transient Luminous Events (TLEs) is the collective name given to a very wide variety of optical phenomena occurring over a wide range of altitudes in the stratosphere,

---

V.P. Pasko (✉)

Department of Electrical Engineering, Communications and Space Sciences Laboratory (CSSL),  
The Pennsylvania State University, 211B Electrical Engineering East, University Park, PA 16802-2706,  
USA  
e-mail: [vpasko@psu.edu](mailto:vpasko@psu.edu)

Y. Yair

Department of Life and Natural Sciences, The Open University of Israel, 1 University Road,  
Ra'anana 43107, Israel  
e-mail: [yoavya@openu.ac.il](mailto:yoavya@openu.ac.il)

C.-L. Kuo

Department of Physics, National Cheng Kung University, No. 1, University Road, Tainan 70101, Taiwan  
e-mail: [johnny@phys.ncku.edu.tw](mailto:johnny@phys.ncku.edu.tw)

and the mesosphere and lower thermosphere, from about 15 to 110 km, in close conjunction with tropospheric electrical activity (e.g., Sentman et al. 1995; Neubert 2003; Pasko 2003, and references cited therein). Although eyewitness reports of TLEs above thunderstorms have been recorded for more than a century, the first image of one was captured in 1989, serendipitously during a test of a low-light television camera (Franz et al. 1990). Since then, several different types of TLEs above thunderstorms have been documented and classified. These include ‘elves’, which are lightning induced flashes that can spread over 300 km laterally (Boeck et al. 1992; Fukunishi et al. 1996; Inan et al. 1991, 1997; Mende et al. 2005; Cheng et al. 2007; Frey et al. 2005; Kuo et al. 2007b); ‘sprites’ that develop at the base of the ionosphere and move rapidly downwards at speeds up to 10,000 km/s (Sentman et al. 1995; Lyons 1996; Stanley et al. 1999; Gerken et al. 2000; Cummer et al. 2006b; McHarg et al. 2007; Stenbaek-Nielsen et al. 2007; Stenbaek-Nielsen and McHarg 2008); ‘halos’, which are brief descending glows with lateral extent 40–70 km, which sometimes (but not always) observed to accompany or precede more structured sprites (Barrington-Leigh et al. 2001; Frey et al. 2007); relatively slow-moving fountains of blue light, known as ‘blue jets’, that emanate from the top of thunderclouds up to an altitude of 40 km (Wescott et al. 1995; Boeck et al. 1995; Lyons et al. 2003); and upward moving ‘gigantic jets’, which establish a direct path of electrical contact between thundercloud tops and the lower ionosphere (Pasko et al. 2002; Su et al. 2003; Pasko 2003; Hsu et al. 2005; Fukunishi et al. 2005; van der Velde et al. 2007, 2010a; Kuo et al. 2007a, 2009; Cummer et al. 2009).

During the two decades elapsed since the original discovery in 1989 several hundred papers have been published in refereed scientific literature reflecting advances in this new and exciting research area. The research activities related to TLEs culminated in a first book, that have appeared in print in 2006 (Fullekrug et al. 2006). Planetary atmospheric electricity aspects relevant to TLEs have been recently covered in the book edited by Leblanc et al. (2008). Early theories of TLEs have been reviewed by Rowland (1998), Sukhorukov and Stubbe (1998) and Wescott et al. (1998). The experimental and theoretical findings related to TLEs have been summarized in several extensive review articles (Boeck et al. 1998; Rodger 1999; Inan 2002; Inan et al. 2010; Lyons et al. 2003; Pasko 2006, 2007, 2008, 2010; Raizer et al. 2010; Neubert et al. 2008; Roussel-Dupre et al. 2008; Mishin and Milikh 2008; Ebert and Sentman 2008; Ebert et al. 2010; Siingh et al. 2008). The goal of the present paper is to provide a limited overview of some of the most recent experimental and modeling developments in studies of TLEs putting emphasis on publications that appeared in refereed literature starting from year 2008 and up to the present date.

## 2 Phenomenology of TLEs and Their Relation to Properties of Lightning and Thunderstorms

The exact nature of the relationship between the properties of the parent thunderstorm that harbored the specific causative lightning flash of the TLE, and the properties of the observed optical emissions have been the basis for numerous works and several comprehensive reviews have already been published (Lyons 2006; Neubert et al. 2008; Pasko 2010). Sprites represent one of the most morphologically complex types of TLEs and in this section we mostly focus on phenomenology of sprites by describing the latest observational results, also pointing to open issues and outstanding questions. Additional information on phenomenology of other types of TLEs is included in Sects. 3 and 4 that follow.

Clearly, not only the source of the rapid change in the above-cloud electrical field plays a part in the formation of sprites: the “initial conditions” existing in the mesosphere and

the ionosphere are undoubtedly important as well (density fluctuations, gravity waves, meteoritic dust), thus leading to an intricate and complicated interplay between the parent flash and the response of the atmospheric medium. Additionally, it is already recognized that sprites sometimes tend to re-appear in regions that had already been occupied by previous sprites, hinting at a local modification of the electrical and chemical properties of the mesosphere at sub-ionospheric altitudes (Haldoupis et al. 2010), thus pre-conditioning and facilitating the emergence of new sprites, pending the occurrence of lightning discharges with sufficient power. Significant progress had been made in quantifying and establishing concrete relations, though as can be expected, due the large variety of thunderstorms and of their lightning flashes, any generalization is bound to be limited and outstanding cases will exist.

## 2.1 Thunderstorms and Lightning Properties Leading to Sprite Formation

### 2.1.1 Meteorology of Sprite-Producing Thunderstorms

Not every thunderstorm produces sprites: rather, it is just a minority of storms that are accompanied by observable optical effects in the upper atmosphere. While the average global flash rate is approximately 44 flashes per second (Christian et al. 2003), the observed global sprite rate based on satellite observations is roughly 1 per minute (Kuo et al. 2008); and see Sect. 4 for a detailed overview). It has long been recognized that positive cloud-to-ground flashes (hereto after +CGs) are responsible for 99% of observed sprites, while negative cloud-to-ground flashes (−CGs) only rarely produce sprites. Since −CGs are overwhelmingly more abundant than +CGs, it is no wonder that sprites are rather scarce, even though lightning is abundant. Another facet to explain this disparity is based on the nature of sprite-producing storms: these are most often the trailing stratiform regions (but not always) of large convective weather systems, which are typically continental in nature. Williams and Yair (2006) have mapped the types of sprite-producing weather systems in summer and winter storms, and noted the differences in size and in charge structure of the thunderstorms in various regions and conditions. Lyons et al. (2009) review the probability of different types of convective storms to generate sprite-halos, sprites and elves. Figure 17.1 in their book-chapter summarizes the different types of thunderstorms. Mesoscale Convective Complexes (MCC), with overall area of cold cloud tops exceeding 100,000 square kilometers and persisting for more than six hours, possesses a “very high” likelihood to generate TLEs, while Mesoscale Convective Systems (MCS) rate second with a “high” likelihood. Winter convection, tropical storms and squall-lines have variable to low probability, while air-mass thunderstorms and super-cells produce sprites only rarely.

### 2.1.2 Parent Lightning Parameters

There are several different parameters which may be used to describe a lightning flash. The most well known are the polarity of the flash, its peak current and multiplicity, the existence of M-components, the magnitude and duration of the continuing current and the resultant charge moment change. It had been recognized that the decisive factor for the generation of sprites is the magnitude of the vertical charge-moment-change (CMC), defined as the product of the charge ( $Q$ ) and the altitude from which it was lowered ( $h_Q$ ) (Cummer et al. 2006b). A similar metric is the impulsive charge-moment-change (iCMC) defined as the total charge moment change within the first 2 ms after the lightning return stroke. Lyons et al. (2009) show that the magnitude of the iCMC for sprite-producing +CGs in the June 20

2007 MCC was always larger than the most commonly occurring +CG, which was typically smaller than 50 C km. Events which had an instantaneous charge moment change larger than 300 C km had a 75% likelihood to generate “an optically detected TLE” (Fig. 17.12, *ibid*). Hu et al. (2002) found that there is a 90% probability for sprite generation by a CMC of 1000 C km (or greater) caused within 6 ms of the parent +CG, and only 10% probability for a CMC of 600 C km or lower. Cummer and Lyons (2005) established a value of CMC of 500 C km as a limit for the generation of short-delayed sprites. Based on ELF data, Greenberg et al. (2007) found CMC values for sprite-producing +CG in eastern Mediterranean winter storms to range from 600 to 2800 C km, with  $\sim 1000$  C km the frequent value. They noted that no significant difference in the ELF signatures and the computed CMCs was found for sprite- and non-sprite producing +CGs, suggesting that other factors play a role in sprite initiation. Lu et al. (2009) analyzed very strong +CG, and showed that even though they had large CMC (1500–3200 C km) they were not accompanied by any TLE. (Li et al. 2008) analyzed summer storms in central US and found that the total CMC ranged from 600 to 18,600 C km. While these values certainly match the concept of removal of charge from a wide area of the storm (Williams 2006), there are cases when even flashes with a CMC as low as 120 C km can trigger sprites (Hu et al. 2002). For winter thunderstorms, sprite producing +CG were found to have average CMC values of  $1400 \pm 600$  C km, with some extreme events exceeding 3500 C km (Yair et al. 2009).

In addition to the CMC of the parent flash, it appears that in-cloud discharge processes preceding the actual attachment of the lightning channel to the ground, and some immediately following the return stroke, also play a role in the formation of sprites and in determining their properties. van der Velde et al. (2006) found distinct differences between in-cloud activity (as indicated by VHF bursts) prior to the generative +CG for column and carrot sprites. While column sprites appear with little or no VHF activity of the parent +CG, carrot sprites are usually associated with a burst of VHF activity, preceding the parent flash by 25–75 ms. Carrot sprites are also found to be associated with intense spherics caused by in-cloud lightning, lasting for 50 to 250 ms after the +CG, hinting at the existence of continuing current in the discharge channel, transferring the cloud charge to the ground. Yashunin et al. (2007) had suggested that the lightning M-components (these are transient surges or fluctuations in the continuing current stage after the first return stroke) may shift the electric field maximum from the location of the vertical channel, facilitating the appearance of delayed and offset sprites. The source of the lateral offset of sprite elements relative to the location of the +CG is still an open question for research. Recently, van der Velde et al. (2010b) analyzed the in-cloud component of the sprite-associated lightning flashes and those of other flashes. They showed that sprite development coincided with VHF bursts of the +CG, and is well correlated with the longest-lasting and largest lateral discharge channel dimensions.

## 2.2 Sprite Morphology

### 2.2.1 Shapes and Sizes of Sprites

There are many types and variations in the shapes and sizes of sprites. Indeed, due to the introduction of high-speed imagery, global satellite observations and advanced computer modeling and laboratory experiments, significant advances in understanding of sprite formation and propagation had been achieved. However, in any discussion of sprite properties, it should be born in mind that although in normal-rate video (which is most commonly used and the major source for the existing data) sprites appear like giant structures spanning large volumes and areas of the atmosphere, in reality such images are merely a “frozen



**Fig. 1** A typical sprite event with multiple elements, with tendrils and bright cores. A large sprite-halo is clearly observed at the upper part. The image was taken by Michal Ganot with a Watec 902H camera at regular video speed, as part of the Eurosprite 2007 campaign in France. Courtesy of the ILAN team

history” of the fast movement of very small and bright volumes of intense ionization in streamer heads (Marshall and Inan 2006). One should also be aware that using 2D images (which in reality are projections of a 3D phenomenon) poses a severe limitation on our ability to fully describe sprites. That handicap can be partly overcome by multiple coordinated observations (e.g., Stenbaek-Nielsen et al. 2010) and using analogies and similarity rules between laboratory streamers and sprites, especially with the latest advances in stereographic imagery of streamers (Nijdam et al. 2008). Sprite shapes can be as simple as a single short vertical column, or can be composed of many distinct, spatially separated elements with a complex mixture of sizes, orientations and shapes. There exists a variety of sprite morphologies resembling straight columns, carrots, jelly-fish or fireworks. This variability necessitated inventing sub-classifications: (i) Columniform sprites (C-sprites) which appear as distinct, thin, vertical and elongated columns of light, either single or multiple (ii) Carrot sprites, which are composed of a heart-shaped central body with numerous protruding convulsed tendrils, resembling leaves or hairs (iii) Jellyfish sprites which are much larger in volume and area, with a big bright body and an overlaying canopy above numerous downward propagating tendrils and (iv) Angle sprites which are bifurcated columns with bright channels extending diagonally. A typical carrot sprite with a halo is given in Fig. 1. In general, one can distinguish between three distinct regions in sprites: the lower streamer region, the bright transition region, and an upper diffuse region (Pasko et al. 1998a; Pasko and Stenbaek-Nielsen 2002). The relative size, brightness and shape of these three regions are manifestations of the discharge process occurring at these altitudes, and can be attributed to the physical mechanisms of streamer generation and propagation that are a

function of the reduced electric field, defined as a ratio of electric field magnitude  $E$  to the air density  $N$ ,  $E/N$  (Ebert and Sentman 2008). Review of recent work on sprite streamers is presented in Sect. 3.2.

### 2.2.2 Time Delays of Sprite from the Parent +CG

Sprites appear in short conjunction after the causative +CG, typically of the order of several milliseconds. The difficulty in establishing the exact time delay is twofold: determining the exact sprite beginning time within the first video frame showing luminosity (typically inducing a 17 ms uncertainty in normal rate cameras), and the relative accuracy of the lightning detection network (usually GPS time-based). Observations in numerous campaigns in the US, Europe, Japan and Israel showed that a dividing time of approximately 10 ms can be defined to distinguish between short- (i.e., immediate, occurring within  $\leq 10$  ms) and long-delayed ( $\geq 10$  ms) sprites. Lyons et al. (2008) state that approximately half of observed sprites are delayed by more than 10 ms after their parent +CG, a fact that exemplifies the role of the continuing current for sprites initiation. Indeed, Li et al. (2008) found that out of 83 sprites they observed, 46% were long-delayed, and analyzed a typical long-delayed event: it was preceded by a +CG with an iCMC of 193 C km, which is below the usual threshold to ignite a sprite. The return stroke was followed by a 144 ms delay until the first sprite luminosity was detected, during which time a continuing current with an average 16 kA flowed, generating an integrated total charge moment change of 2650 C km. This event shows that it is not necessarily the iCMC which is important, but rather, the total CMC. In summer storms in Europe, van der Velde et al. (2006) reported that column sprites occur with a short time delay ( $< 30$  ms) from the causative +CG, while carrots are usually delayed up to  $\sim 200$  ms relative to their causative +CG stroke. Similar results were reported by Yair et al. (2009) for winter thunderstorms in the Eastern Mediterranean: the average time delay between the ELF transient of the parent +CG and the observed sprites was 55 ms, with shorter delays for column sprites ( $42 \pm 17$  ms) compared to carrot sprites ( $68 \pm 17$ ). Matsudo et al. (2009) compared time delays of sprites in winter storms in the Hokoriku region of western Japan. The most common sprite shape in this type of storms is simple vertical columns (68%) and the average delay time was found to be 90 ms. Similar winter storms over the Pacific Ocean east of Japan show delayed sprites by 43 ms on average.

### 2.2.3 Onset Altitudes

From the considerations of Wilson's theory (Wilson 1925), there exists an altitude in the atmosphere where the thunderstorm-induced electric field should surpass the conventional breakdown field (see Fig. 2 in Pasko 2010). Since the breakdown field is proportional to air density, it follows that sprites will initiate at altitudes where electric field can be sustained against fast relaxation in the highly conducting ionosphere and where the density of air is sufficiently low: between 75 and 80 km for typical conditions. Most of existing observations conducted with regular speed video have difficulty in determining the exact onset altitudes of sprites because of inaccuracies in range determination to the observed emissions, whose initial stages may be missed due to sensitivity issues. Range inaccuracy is inherent in single-station observations (even with star-field alignment) and in part stems also from the fact that sprites are often offset with respect to the ground location of the parent flash (which is precisely known based on lightning detection network data). In spite of these limitations, the determined altitudes range between 75 and 85 km agree with Wilson's predictions, where sprites seem to initiate and propagate. Figure 2 shows a sprite initiating from



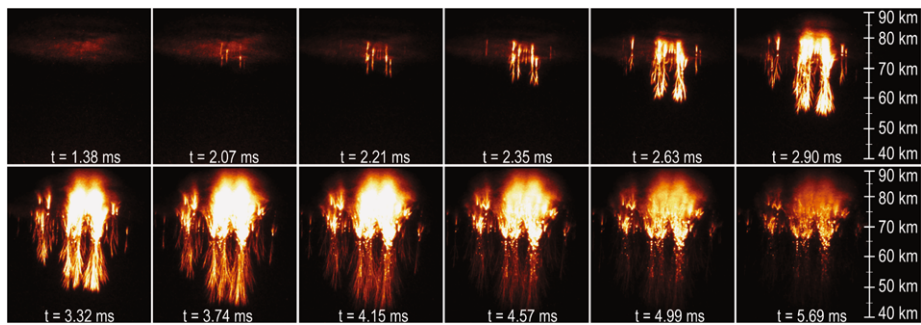


**Fig. 2** The evolution of sprite streamers as depicted by high-speed imagery. The sprite emerges from the bottom of a diffuse glow (halo) and develops downward in visible complex tendrils. The uppermost main body of the sprite obtains a diffuse appearance. Courtesy of Steve Cummer, Duke University

a dim halo at 80 km, and propagates in several separate tendrils extending all the way down to 45 km. This observation of a dim halo at  $\sim 85$  km preceding the appearance of streamers by Cummer et al. (2006b) was later modeled by Luque and Ebert (2009), as discussed in Sect. 3.2. High-speed (10,000 Hz) triangulated imagery by Stenbaek-Nielsen et al. (2010) showed that inception altitudes of the downward motion of sprite streamers is between 66 and 89 km, while in those cases where an upward streamer motion is found to occur (with a slight delay after the initial downward phase), it starts at lower altitudes: 64 to 78 km. This initiation may be related to negative charging of sprite elements (Luque and Ebert 2010; Li and Cummer 2011), as will be further discussed in Sect. 3.2. Gamera et al. (2011) used a similar technique to compare observed and modeled sprite initiation altitudes. They analyzed 20 discrete sprite events and found that long-delayed sprites initiate at lower altitude. The average discrepancy between the measurements and their model simulation results was 0.35 km with a standard deviation of 3.6 km.

#### 2.2.4 Sizes of Sprite Elements

The length of sprites is a measure of the overall duration of the movement of the streamer heads in the ambient electric field. High-speed imagery (Marshall and Inan 2006; McHarg et al. 2007; Stenbaek-Nielsen and McHarg 2008; Montanya et al. 2010) shows that sprites are composed of numerous compact, very fast ( $\sim 10^7$  m/s) downward moving elements, that become brighter as they descent. The sizes of each individual streamers head are between tens to hundreds of meters and they leave a narrower trail in their wake. Telescopic observations by Gerken and Inan (2003) reported decametric structures in sprites. As mentioned above, the movement of streamer heads (sometimes referred to as “tendrils”) as recorded by regular-speed video creates the illusion of elongated, vertical columns of light, and so any discussion of the vertical dimension of sprites actually reflects the time-integrated motion of these elements, clearly exemplified by Ebert et al. (2006) in the analogy to laboratory streamers at different time-exposures. Stenbaek-Nielsen and McHarg (2008) use the term “confetti falling from the sky” to describe this motion, as there are numerous such elements forming a single sprite. Relevant modeling results are described in Sect. 3.2. It should also be pointed out that in many cases, an upward movement of streamers is observed, 0.5–2 ms after the onset of the downward motion, with speeds slightly faster than the downward motion ( $\sim 6 \times 10^7$  m/s). These upward streamers also possess a horizontal velocity component which leads to spreading out on a large scale, which creates the typical

shape of carrot sprites. In column sprites, such upward streamers are not observed, and a simpler shape is maintained.

### 2.2.5 Spatial Organization of Sprite Elements

Sprites can span a large horizontal dimension, and impact a considerable volume of the mesosphere. Since almost all existing images offer only a 2-dimensional view of sprites, we lack a full mapping in 3 dimensions of their organization. In this regard we note that the first color imagery of sprites and their unambiguous physical dimensions and heights were obtained using triangulation from two jet aircraft (Sentman et al. 1995). Recent triangulation studies provided valuable information about initiation altitudes of downward (66 to 89 km) and upward (64 to 78 km) streamers, that associate with formation of columnar (C sprites) and carrot sprites, respectively (Stenbaek-Nielsen et al. 2010). Stanley et al. (2007) mapped sprite locations and compared them to LMA-derived flash dimensions and reported that sprites were arranged preferably on the periphery of the discharge. Vadislavsky et al. (2009) showed that in some cases, sprite elements appear to be organized in a circular shape above, or slightly offset, to the +CG location. Inan (personal communication, 2008) suggested that previous IC flashes lead to the creation of an attachment dominated “hole” of electron concentration at the region above the +CG, which prevents sprite formation directly above the +CG. Another possibility was suggested by Adachi et al. (2004), based on the circular shape of the lightning-induced EMP, that acts to pre-empt the mesosphere before the ensuing quasi-static electric (QE) field. van der Velde et al. (2010a) found that the propagation of the lightning channel during a VHF burst dictated the order of appearance of sprite elements, much like the early report by Stanley (2000). The cause of the arrangement of the different elements in sprites remains unclear.

## 3 Physical Mechanisms and Modeling TLEs

### 3.1 Interaction of Lightning Electromagnetic Pulses with Ionosphere and Elves

Inan et al. (1991) were first to predict that lightning might directly affect the lower ionosphere, producing both ionization and optical emissions which we know as elves phenomenon. After their initial discovery from the Space Shuttle (Boeck et al. 1992) the first ground observations of elves were made by Fukunishi et al. (1996) and Inan et al. (1997) using photometers. The summary of important historical facts and processes related to research on interaction of lightning induced electromagnetic pulses (EMPs) with the lower ionosphere have been given in recent review by Inan et al. (2010).

Inan et al. (1997) predicted that based on radiation pattern of a vertical cloud to ground lightning discharge, considered to be acting as a linear antenna element, the optical luminosity of elves should have a donut shape with a distinct minimum right above the causative discharge. Kuo et al. (2007b) recently performed detailed in-depth study of elves recorded by the ISUAL instrument on FORMOSAT-2 satellite. The modeling component of that study included validation of elves modeling indicating good agreement for: direct comparison of photon fluxes calculated by the model and observed by ISUAL spectrophotometers, direct comparison of modeled and observed morphologies of elves, and direct comparison of the calculated photon fluxes using peak currents for two elve-associated NLDN cloud to ground lightning discharges with those recorded by the ISUAL Imager (Kuo et al. 2007b). Figure 3 illustrates modeling results obtained in Kuo et al. (2007b) that are in excellent agreement



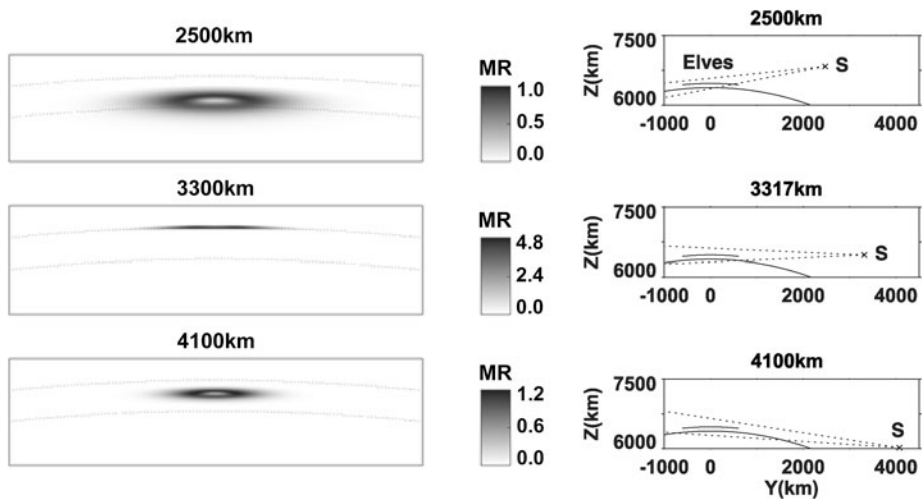


**Fig. 3** Optical emissions of first positive band system of  $N_2$  of a modeled elve (peak current 280 kA) in front (2500 km), at (3300 km) and behind (4100 km) the limb (Kuo et al. 2007b). Reprinted by permission from American Geophysical Union

with observed morphological features of elves recorded by the ISUAL under different viewing conditions, when elves appear in front, at, or behind the limb.

Marshall et al. (2010) have recently presented a three-dimensional finite difference time domain model for simulation of the lightning electromagnetic pulse and its interaction with the lower ionosphere. The results agree with the frequently observed, doughnut-shaped optical signature of elves, as illustrated by Fig. 3, but also show that the structure exhibits asymmetry due to the presence of Earth's ambient magnetic field. This prediction has not yet been confirmed by experiment. Additional quantitative results presented in Marshall et al. (2010) indicate that in-cloud (horizontal) lightning channels produce observable optical emissions without the doughnut shape and, in fact, produce a much stronger optical output for the same lightning current. Results of modeling of a realistic burst of in-cloud lightning activity, that involved series of pulses with realistic pulse amplitudes and random altitudes and orientations, produced an electron density increase of over 200% in the overlying ionosphere. Marshall and Inan (2010) further indicated that these factor of two increases in local density associated with elves yield small but detectable perturbations to the sub-ionospherically propagating very low frequency (VLF) transmitter signals and may explain at least some observed perturbations produced by direct interaction of lightning electromagnetic emissions with the lower ionosphere known as early/slow VLF events (see also recent work by Haldoupis et al. (2009) and Haldoupis et al. (2010) that include extensive list of references documenting the phenomenology of early VLF events in connection with sprites and elves, as reported by Mika et al. (2006)).

Lay et al. (2010) have recently performed a modeling study of cumulative effects of a sequence of strong lightning discharges on the lower ionosphere. The study involved a sequential application of ten lightning discharges with peak current 150 kA and rise time 20  $\mu$ s. The stroke rates were based on World-Wide Lightning Location Network measurements. The study employed a two-dimensional axisymmetric finite-difference time-domain model that describes the effect of lightning electromagnetic pulses on the ionosphere. The authors noted an interesting effect of successive electromagnetic pulses in which each pulse inter-

acts with a modified background ionosphere due to the previous pulses. In reported results a formation of nonlinear electron density perturbation over time, that eventually reached a limiting value, was observed. The limiting maximum electron density was reached earlier in time for higher altitudes, and the most significant effect occurred at 88 km. The limiting modeled electron density profile in the 83–91 km altitude range did not depend on the initial electron density (Lay et al. 2010). The effect of steepening of the ambient electron density profile reported by Lay et al. (2010) may have a direct facilitating effect on initiation of sprite streamers as discussed recently in Qin et al. (2011, see Fig. 9 and associated text).

### 3.2 Modeling of Sprites

#### 3.2.1 Modeling of Large Scale Electrodynamics of Sprites

The charge moment change  $Qh_Q$  (i.e., charge removed by lightning  $Q$  times the altitude from which it was removed  $h_Q$ ) represents the key parameter which is used in current sprite literature to measure the strength of lightning in terms of sprite production potential (Cummer et al. 1998; Hu et al. 2002, 2007; Li et al. 2008; Cummer 2003; Cummer and Lyons 2004, 2005; Cummer et al. 2006a). Computer simulations of Hiraki and Fukunishi (2006) and Asano et al. (2008) also indicate importance of the product of the current ( $Ih_Q$ ) and charge ( $Qh_Q$ ) moments for sprite initiation and suggest the threshold value:  $(Ih_Q) \times (Qh_Q) = 1.6 \times 10^6$  (A km)(C km). The results of Hiraki and Fukunishi (2006) and Asano et al. (2008) emphasize importance of the timescale of charge removal by lightning for initiation of sprites. These conclusions are generally in agreement with analysis reported in Barrington-Leigh et al. (2001) indicating that a lightning discharge with a fast ( $<1$  ms) charge moment change may be sufficient to cause diffuse emissions at higher altitudes, where the threshold for ionization and optical excitation is lower. If lightning currents do not continue to flow, however, there may not be sufficient electric field to initiate streamers below  $\sim 75$  km. Conversely, slow continuing currents may cause a (delayed) sprite without a significant initial flash in the diffuse (halo) region (Barrington-Leigh et al. 2001).

In recent years the ELF measurements of the time dynamics of the charge moment changes in sprite-producing lightning have progressed to the point allowing detailed event based testing of sprite theory (Hu et al. 2007; Li et al. 2008). The modeling analysis reported by Hu et al. (2007) provided quantitative information on time variation of lightning current moment, charge moment and electric field driving sprite phenomena and demonstrated that for bright, short-delayed sprites, the measurement-inferred mesospheric electric field agrees within 20% with the threshold electric field for conventional breakdown  $E_k$ . However, for long delayed sprite events and dimmer sprites, the measurement-inferred mesospheric electric field for sprite initiation is somehow below  $E_k$  values (Hu et al. 2007). Figure 4 shows measured current and charge moments and the simulated electric fields between 50 and 90 km altitude (normalized by  $E_k$ ) for the typical long-delayed sprite (Li et al. 2008). The sprite is initiated at 144.4 ms after the lightning return stroke. The electric field increased before the sprite onset due to slow intensification of the continuing current. The peak normalized electric field in Fig. 4b producing the long-delayed sprite is  $E/E_k = 0.45$  at 72 km altitude, which is similar to those for typical short-delayed sprites that are neither remarkably bright or dim (Hu et al. 2007). The modeled initiation altitude of 72 km falls in the 70–80 km range estimated from high-speed video images (Li et al. 2008). Comparison of modeling and observations indicate that the long-delayed sprites initiate 5 km lower than short-delayed sprites (Li et al. 2008). The results of Li et al. (2008) have recently been confirmed using analysis of 20 additional discrete sprite events (Gamerota et al. 2011). The

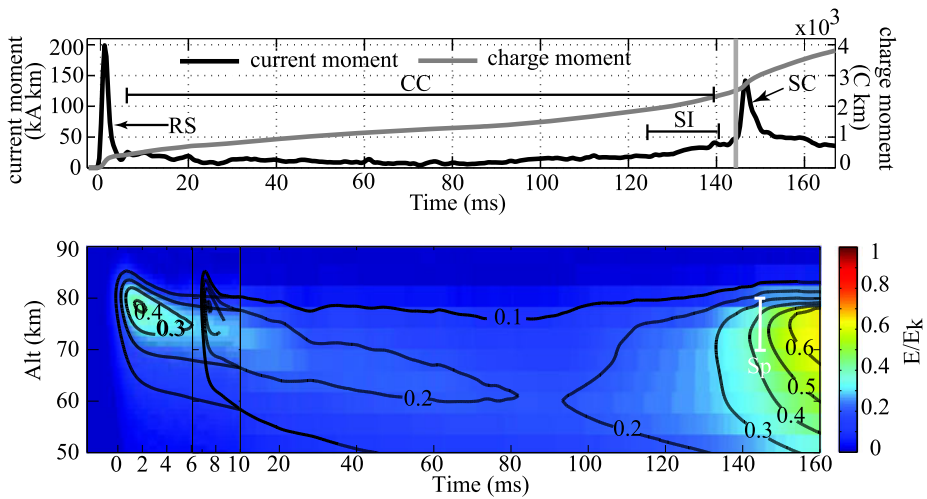


**Fig. 4** Finite difference time domain (FDTD) simulation results for the typical long-delayed sprite event (Li et al. 2008). (a) Estimated current moment and total charge moment change. (b) Simulated electric fields above the lightning discharge. Reprinted from Li et al. (2008) by permission from American Geophysical Union

comparisons of 2D FDTD model results and observations indicate good agreement between measured and modeled initiation altitudes (defined on the basis of peak  $E/E_k$  values), with average discrepancy of 0.35 km with a standard deviation of 3.6 km.

Adachi et al. (2008) combined array photometer data obtained by ISUAL instrument on FORMOSAT-2 satellite with the ELF magnetic field data to deduce temporal evolutions of lightning charge moment changes driving sprites and halos. It was found that the lightning discharge producing a halo without streamers has a short time scale of  $\sim 1$  ms with a moderate charge moment of  $Qh_Q \sim 400$  C km while that producing streamers as well as a halo have a similar time scale of  $\sim 1$  ms but a large charge moment of  $Qh_Q \sim 1300$  C km. On the other hand, a lightning discharge producing sprite streamers without a discernible halo has a long time scale of  $\sim 10$  ms and a large charge moment of  $\sim 1300$  C km. These conclusions are in agreement with results reported in Barrington-Leigh et al. (2001), Hiraki and Fukunishi (2006), Asano et al. (2008).

Lightning M components are perturbations or transient enhancements in the continuing current (Rakov et al. 2001). Rakov et al. (2001) speculated that M-component type processes in positive lightning may play a role in the initiation of so-called delayed sprites that occur many tens of milliseconds after the return stroke. Modeling analysis of Yashunin et al. (2007) indicates that the occurrence of an M component shifts the electric field maximum from the vertical axis of the lightning channel and increases the likelihood of initiation of sprites spatially displaced with respect to the lightning channel axis. Asano et al. (2009b) established through computer simulations that M components in the continuing current with small amplitudes but fast time variations can initiate or enhance the occurrence of sprites. Asano et al. (2009a) utilized three-dimensional fully electromagnetic simulations to investigate effects of horizontal components of currents in lightning discharges in addition to the conventional vertical channel. It has been established that the position of sprite can be significantly shifted in response to the length of the horizontal lightning channel due to additional ionization effects created by electromagnetic pulse radiation from the horizontal channel (Asano et al. 2009a).

### 3.2.2 Modeling of Sprite Streamers

Significant efforts in recent years have been devoted to modeling of fine streamer structures in sprites and their interpretation. Streamers are needle-shaped filaments of ionization embedded in originally cold (near room temperature) air and driven by strong fields due to charge separation in their heads (Raizer 1991, p. 334). The streamer polarity is defined by the sign of the charge in its head. The positive streamer propagates against the direction of the electron drift and requires ambient seed electrons avalanching toward the streamer head for the spatial advancement (Dhali and Williams 1987). The negative streamer is generally able to propagate without the seed electrons since electron avalanches originating from the streamer head propagate in the same direction as the streamer (Vitello et al. 1994; Rocco et al. 2002). A detailed review of various properties of streamers, including fields required for their initiation and propagation, and similarity relationships allowing scaling of streamer parameters as a function of gas pressure for the purposes of interpretation of sprite discharges, is provided in Pasko et al. (1998a), Pasko (2006, 2007, 2008). Below we review related recent work directed to the modeling interpretation of sprite observations.

First particle simulations of sprite streamers have been reported by Chanrion and Neubert (2008). The code is in 2D axi-symmetric coordinates with charged particles followed in a Cartesian mesh and the electric field updated with Poisson's equation from the charged particle densities. Collisional processes between electrons and air molecules are simulated with a Monte Carlo technique, according to cross section probabilities. The code also includes photoionization processes of air molecules by photons emitted by excited constituents. Chanrion and Neubert (2008) presented detailed comparisons of results from the new particle model with previous fluid model of Liu and Pasko (2004) for the case of double headed streamers developing at 70 km altitude in air using identical initial plasma, electric field and neutral atmosphere parameters. The results demonstrated excellent agreement with the previous fluid modeling. It is shown that at 1 atm pressure the electric field must exceed similar to 7.5 times the breakdown field to observe runaway electrons in a constant electric field. It is also found that this value is reached in a negative streamer tip at 10 km altitude when the background electric field equals similar to 3 times the breakdown field. It is shown that the energetic runaway electrons produced by streamer tips create enhanced ionization in front of negative streamers. The simulations suggest that the thermal runaway mechanism may operate at lower altitudes and be associated with lightning and thundercloud electrification while the mechanism is unlikely to be important in sprite generation at higher altitudes in the mesosphere (Chanrion and Neubert 2008). The model of Chanrion and Neubert (2008) has recently been extended with an improved description of high-energy electrons in Chanrion and Neubert (2010).

The electric fields associated with streamer discharges in TLEs are now routinely measured considering the ratios of spatially integrated radiation intensities of band systems with different energy excitation thresholds (e.g., Kuo et al. 2005, 2009; Liu et al. 2006, 2009b; Adachi et al. 2006). In a streamer, the head is usually responsible for the most part of ionization and excitation of species, and therefore is responsible for the most part of emission. However, the spatial non-uniformity of streamer discharges is such that the maximum excitation rates are not exactly located at the spatial position of the maximum electric field (Naidis 2009). Following recent work by Naidis (2009), Celestin and Pasko (2010) demonstrated that due to strong spatial variations of the electron density and electric field in streamer heads previous measurements may lead to a significant underestimation of the peak values of electric fields in TLEs. The modeling analysis of streamers as a function of altitude, applied reduced electric field, and streamer polarity conducted by Celestin and Pasko (2010) indicated

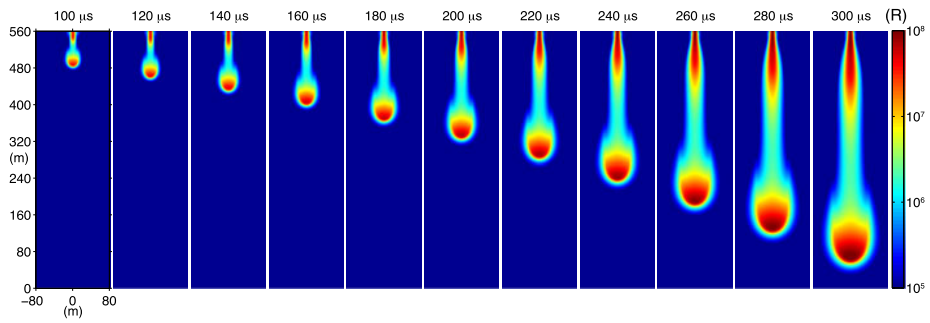


**Fig. 5** A time sequence of intensity distributions of first positive band system of  $N_2$  for a downward propagating model positive streamer at 75 km altitude (Liu et al. 2009a). The sequence of images is shown with 20- $\mu$ s interval, starting at 100  $\mu$ s and ending at 300  $\mu$ s. The formatting is consistent with that of Stenbaek-Nielsen et al. (2007, Fig. 2). Reprinted by permission from American Geophysical Union

that the ratios based electric fields derived from spectrophotometric data need to be multiplied by a corrective factor  $> 1.4$  for positive streamers and  $> 1.5$  for negative streamers, to obtain the true peak values of electric fields. The study of Celestin and Pasko (2010) brings the values of electric field previously deduced from observations (e.g., Kuo et al. 2005; Adachi et al. 2006) much closer to streamer simulations. Moreover, one can note that the value  $5.5E_k$  documented in Kuo et al. (2009) for negative gigantic jet discharge would lead to the very high field  $> 1.5 \times 5.5E_k \simeq 8E_k$  approaching or exceeding magnitudes for which thermal electron runaway process becomes possible (e.g., Moss et al. 2006; Li et al. 2009; Chanrion and Neubert 2008, 2010; Celestin and Pasko 2011). These results, therefore, have direct implications for production of runaway electrons in jet discharges.

Liu et al. (2009a) compared sprite streamer modeling results with high-speed video recordings of sprites made with 50  $\mu$ s temporal resolution (McHarg et al. 2007; Stenbaek-Nielsen et al. 2007). Both the modeling results and the sprite videos show that sprite streamers propagate with acceleration and expansion during the initial stage of sprite development. The acceleration computed from the modeling for the applied electric fields close to the conventional breakdown threshold field  $E_k$  is on the order of  $(0.5\text{--}1) \times 10^{10} \text{ m s}^{-2}$  and is in good agreement with the peak values observed experimentally. Mainly due to the increasing radius of the streamer head of an accelerating streamer, the brightness of the streamer head increases as well (see Fig. 5). The results reported in Liu et al. (2009a) demonstrate that the brightness of a sprite streamer head increases exponentially with time and can span more than 4 orders of magnitude in a very short period of about 1 ms. The rate of increase depends on the magnitude of the applied electric field. Liu et al. (2009a) proposed a method for remote sensing of the sprite-driving electric field in the mesospheric and lower ionospheric region by measuring the rate of the change of the brightness. In particular, Liu et al. (2009a) report that the sprite event presented in MchHarg et al. (2007), Stenbaek-Nielsen et al. (2007) was initiated by fields close to the conventional breakdown threshold  $E_k$ .

We note that the exponential expansion and acceleration of streamers is an important effect that was recently identified to be also accompanied by exponential growth of electric potential differences in the streamer heads (Celestin and Pasko 2011). These electric potential differences have significant implications for the energy that thermal runaway electrons can gain once created and quantitative results of Celestin and Pasko (2011) indicate that under realistic conditions associated with lightning leaders streamers can create  $\sim 100$  keV electrons capable of further acceleration to several MeVs energies needed for explanation of

terrestrial gamma ray flashes (TGFs) in the Earth's atmosphere (e.g., Fishman et al. 1994; Smith et al. 2005). We note that the energy of photons in TGFs can reach up to 100 MeV (Tavani et al. 2011), and the most recent observations indicate that many TGFs are produced during upward negative leader progression prevalent in normal polarity intra-cloud flashes (Lu et al. 2010, 2011a).

Although it has been suggested that sprites may be initiated through simultaneous up and down propagating streamers (Liu and Pasko 2004), the recent observational evidence indicates that the preferential form of sprite initiation is through downward development of positive streamers launched in the region of the lower ledge of the Earth's ionosphere (see discussion in Stenbaek-Nielsen et al. 2007). The exact mechanism of initiation of sprite streamers is not well understood and related recent studies are reviewed below. The mechanism may be related to formation of upwardly concave ionization regions near the lower ionospheric boundary associated with sprite halos (Barrington-Leigh et al. 2001). As was discussed recently in Pasko (2010) the double headed streamers may be involved in initiation of sprites, however, due to the fast exponential increase in streamer brightness in time (see review of Liu et al. 2009a above) the initial appearance of positive streamers is likely realized because of a relatively slow application of the electric field at sprite altitudes (1 ms) (Marshall and Inan 2006; Hu et al. 2007) coupled with lower propagation threshold for positive streamers in comparison with negative ones (Pasko et al. 2000), which creates asymmetric conditions with predominant initial propagation of positive streamers. Other factors have also been proposed and review of recent research work on this subject is provided below.

Luque and Ebert (2009) have recently reported a high resolution modeling of inception of sprite streamers as a result of sharpening and collapse of screening-ionization wave associated with sprite halo. The streamer emerged as a result of halo dynamics on the axis of symmetry in a two-dimensional axisymmetric plasma fluid model that employed a non-uniform, dynamically adapted computational grid (Luque and Ebert 2009). The transverse dimension of the modeled streamer was on the order of 1 km, and its time dynamics was resolved on a fine grid with 3 m spatial resolution (Luque and Ebert 2009). This result is qualitatively similar to the dynamics reported in early low resolution sprite modeling in which columns of ionization with transverse extent on the order of 10 km were observed to emerge from upwardly concave regions of sprites and to propagate down to altitudes  $\sim 45$  km (Pasko et al. 1996). We note that although the upwardly concave regions of luminosity forming during sprite development were fully resolved and quantitatively described in early papers (Pasko 1995, 1996, 1997; Veronis et al. 2001) the name sprite halo, that is now used in association with these events, was introduced several years later when these events, driven primarily by quasi-static electric fields, were discovered, clearly identified and separated from elves phenomenon using comparisons of high speed video observations and fully electromagnetic modeling (see discussion in Barrington-Leigh et al. 2001, and references cited therein). A significant difficulty of both the early (Pasko et al. 1996) and more recent (Luque and Ebert 2009) modeling is that streamers appear in these models as a continuous process of halo development, while in many existing high resolution photometric and video records the sprite streamers exhibit significant spatial (both vertical and horizontal) as well as temporal separations with respect to position and timing of the sprite halo (Qin et al. 2011, and extensive list of references therein). The asymmetry in initiation of sprite streamers by cloud-to-ground lightning discharges with different polarities, and sprite streamers triggered by cloud-to-ground lightning with very low charge moment changes are also not reproduced by models reported in Pasko et al. (1996), Luque and Ebert (2009). Additionally, Qin et al. (2011) recently indicated that the collapse of sprite halo reported in Pasko et al. (1996), Luque and Ebert (2009) is due to numerical instability, that can be somewhat postponed but not eliminated by increasing resolution of numerical grid.



Liu (2010) has recently discussed mechanisms for the luminous trail or ‘afterglow’ region often observed at higher altitudes in downward propagating sprite streamers (McHarg et al. 2007; Stenbaek-Nielsen et al. 2007). The physical mechanisms of the observed phenomenon discussed in the existing literature include emissions produced due to energy transfer from  $N_2$  and  $O_2$  metastable electronic states, energy pooling between low energy metastable states, and energy pooling between the metastable states and the vibrationally excited ground electronic state of  $N_2$  (e.g., Morrill et al. 1998; Bucseli et al. 2003; Kanmae et al. 2007; Pasko 2007; Sentman et al. 2008; Sentman and Stenbaek-Nielsen 2009). Liu (2010) demonstrates that the luminous trail also naturally appears in numerical modeling of sprite streamers in which the above-mentioned chemical processes are not taken into account. The effect is due to increase in current that flows in the sprite streamer body when streamer expands, accelerates and brightens. The increasing current self-consistently leads to the rise of the electric field in the streamer channel far behind the streamer head, which leads to effective production of  $N_2$  excited states by electron impact excitation and then to the glowing trail (Liu 2010).

The results of Liu (2010) concerning the luminous trail are in agreement with more recent work (Luque and Ebert 2010) whose authors applied a model with adaptively refined grids to study propagation of long sprite streamers with transverse dimension on the order of 1 km through altitude range with significant variation of ambient air density. Luque and Ebert (2010) observed that in their model the optical emission intensity varied proportionally to air density and therefore exponentially in time for the streamer with velocity and radius that remained relatively stable. The authors also observed a negative charging of the upper section of the positive streamer that propagated downward, and suggested that this negative charging may facilitate emergence of upward negative streamers and attraction of positive streamer heads to previously formed channels as observed experimentally (Luque and Ebert 2010, and references therein).

Li and Cummer (2011) have recently used lightning-driven background electric fields at mesospheric altitudes deduced from ELF electromagnetic measurements in combination with high-speed images of sprite streamers to estimate charges present in bright columnar cores appearing at upper extremities of sprites. The analysis assumed that the observed negative streamers that emerge from the bright negatively charged cores propagate along the directions of the local electric field lines, and the amount and vertical distributions of charge were iterated until good agreement was achieved with high-speed video images in terms of angles of emergence of negative streamers with respect to the vertical cores. The authors were able to establish a lower bound on the electric charge in six observed sprites driven by positive lightning. They found, in particular, that individual bright sprite cores contain significant negative space charge between  $-0.01$  C and  $-0.03$  C. Given the significant negative charge, Li and Cummer (2011) interpreted the sprite core region as the partial and perhaps dominant sink of the negative charge created by the downward positive polarity streamers. This further suggests that when downward streamers supply more charge than can be absorbed by the sprite core, slightly delayed upward negative streamers initiate from the sprite core to disperse this charge (Li and Cummer 2011). This is consistent with observations that show that the subsequent upward streamers are not always present, especially in smaller sprites Li and Cummer (2011). The findings of Li and Cummer (2011) that the emergence of secondary negative streamers may be related to the negative charging of the upper section of the downward positive streamer are consistent with similar ideas advanced in Luque and Ebert (2010). An important original finding of the analysis of Li and Cummer (2011) is that it allowed for the first time to use sprite imagery to find if approximately 10 km long bright sprite core regions were electrically attached to the high conductivity regions of the lower

ionosphere. The analysis indicated a weak or nonexistent electrical connection between the ionosphere and the downward streamer (Li and Cummer 2011). In addition to other important factors discussed above in the context of halo-streamer transition (Pasko et al. 1996; Luque and Ebert 2009), the new findings of Li and Cummer (2011) also support the idea that sprite streamers do not represent a continuous process of sprite halo development as they appear to be electrically disconnected from the upper high conductivity regions of the Earth ionosphere.

In order to monitor the inception of sprite streamers, that cannot be modeled with present computer resources in the framework of fluid models, Qin et al. (2011) have used an improved avalanche-to-streamer transition criterion, and have investigated the response of the lower ionosphere to the charge moment changes induced by lightning discharges as a system of avalanches. Qin et al. (2011) established a direct link between the charge moment change and the ambient electron density profile as required for triggering of sprite streamers. The related condition is defined as  $h_{\text{tran}} \geq h_{\text{cr}}$ , where  $h_{\text{tran}}$  represents the altitude at which the electron density is low enough so that the distance between electrons is equal to the radius of the electron avalanche at the moment of avalanche-to-streamer transition, and  $h_{\text{cr}}$  represents the altitude at which the ambient electric field  $E_{\text{amb}}$  created by the charge moment change in the thunderstorm is equal to the conventional breakdown field  $E_k$  defined by the equality of ionization and dissociative attachment frequencies in air. An analysis of the origin of polarity asymmetry between +CGs and -CGs in triggering of sprite streamers conducted by Qin et al. (2011) indicated that the vertical extent of streamer initiation region (SIR) created by a -CG was smaller than the SIR created by the opposite +CG that corresponded to the same charge moment change. This is due to the fact that, the positive SIR is basically equivalent to the high field  $E > E_k$  region created by the halo because upward avalanches generated in a low electron density region can penetrate deep into the high electron density region of the halo. In contrast, the negative SIR is limited to the high field region where the electron density is low enough for avalanches to develop without overlapping. Qin et al. (2011) also demonstrated as part of the asymmetry study that the triggering of long-delayed sprites is a unique property of halos produced by positive cloud-to-ground lightning discharges due to the formation of a long-lasting high field region, that can be significantly enlarged by the lightning continuing current. Qin et al. (2011) demonstrate importance of initial inhomogeneities in the lower ionosphere for initiation of sprite streamers and indicate that a large number of initial seed electrons distributed in a compact region of space  $N_{0e}$  creates more favorable conditions for initiation of sprite streamers. It is important to emphasize that the initial inhomogeneities were discussed in many early papers on sprite modeling (Pasko et al. 1996, 1997; Raizer et al. 1998, 2010; Zabolotn and Wright 2001). Raizer et al. (1998, 2010), for example, introduce a seed inhomogeneity with radius 60 m and electron density  $150 \text{ cm}^{-3}$  (corresponding to  $N_{0e} \sim 10^{14}$ ) at 80 km altitude. The approach of Qin et al. (2011) is different as it considers the seed electrons in the framework of competition of many avalanches in which only a perturbation with a larger number of initial electrons reaches the avalanche-to-streamer transition, becomes dominant in defining the macroscopic electric field, and also eventually becomes observable. Qin et al. (2011) quantitatively demonstrate that in the framework of avalanche-to-streamer transition even values twelve orders of magnitude lower than those employed by Raizer et al. (1998, 2010) (i.e.,  $N_{0e} \sim 10^2$ ) play a definitive role in initiation of sprite streamers. The possible role of inhomogeneities in electron density in formation of bright beads and branching of sprite streamers has recently been discussed by Luque and Gordillo-Vazquez (2011).

### 3.3 Modeling of Jets

A summary of phenomenological features of blue jets and gigantic jets and their proposed relationship to different polarity leader processes has been presented recently in Pasko (2008). Assuming that both types of jets originate from streamer zones of conventional lightning leaders propagating upward from thundercloud tops, the continuous positive leader-like propagation of optically observed blue jets should be contrasted with the impulsive rebrightening of gigantic jets, resembling negative leader processes (Krehbiel et al. 2008). The polarity itself is not sufficient to explain all the morphological differences in jet events observed to date. In particular, Krehbiel et al. (2008) emphasize that the location of jet initiation and charge configuration in a thundercloud are also defining parameters for jet development. Although the discussion presented in recent reviews by Pasko (2008) and Pasko (2010) suggests association of blue jets with positive leaders and gigantic jets with negative leaders, the recent observations of a positive gigantic jet exhibiting similar morphological features to those in previously documented negative gigantic jets (van der Velde et al. 2010a) indicate that the situation is more complicated than originally thought. Extensive discussion on possible classification schemes of different jet events is given in Krehbiel et al. (2008) (see also Supplementary Information for Krehbiel et al. 2008 available on *Nature Geoscience* web site). We note that van der Velde et al. (2010a) indicated that there was an evidence that the positive gigantic jet was produced by an inverted polarity storm. This appears to be in excellent agreement with predictions of Krehbiel et al. (2008) of positive gigantic jets produced by inverted polarity storms (i.e., storms in which main negative charge is located above the main positive charge).

Raizer et al. (2006, 2007, 2010) associated both blue jets and gigantic jets with the streamer zone of positive leader, which is postulated to be initiated above the positive charge center positioned at altitude 12 km. Raizer et al. (2006, 2007, 2010) demonstrated that upward transfer of the high thundercloud potential by leader channel to lower air density regions with proportionally lower electric field threshold for propagation of streamers  $E_{cr}^+$ , allowed the sustainment of blue jet streamers by relatively moderate cloud charge of 50 C with a radius of 3 km.

Milikh and Shneider (2008) utilized the modeling approach proposed in Raizer et al. (2007) to study 300–400 nm emissions produced by a jet discharge in order to interpret flashes with 1–64 ms duration observed in equatorial regions by UV instrument on board of the microsatellite ‘Tatiana’. The modeling considered the second positive band system of  $N_2$  and the first negative band system of  $N_2^+$  as primary emissions responsible for the observed flashes and accounted for excitation as well as for pressure dependent quenching effects of the responsible electronic states  $C^3\Pi_u$  of  $N_2$  and  $B^2\Sigma_u^+$  of  $N_2^+$ , respectively. The model calculated UV fluxes are in agreement with those observed in terms of UV pulse duration and magnitude (Milikh and Shneider 2008).

In addition to an obvious disagreement with the inferred negative polarity of some of the gigantic jets observed to date, the limitation of models proposed in Pasko et al. (1999), Pasko and George (2002), Raizer et al. (2006, 2007, 2010) in support of the original idea expressed by Petrov and Petrova (1999) that jets correspond to the upward development of the pressure scaled streamer zone of a conventional leader is that they all postulate presence of a leader near the cloud top. These models do not provide a link to experimentally documented charge distributions and lightning phenomenology in thunderstorms leading to the initiation and upward escape of the leader process from the thundercloud top. There is experimental evidence, for example, that some of the gigantic jets are initiated as normal polarity intra-cloud lightning discharges between upper positive and lower negative charge

centers (Mathews et al. 2002; Krehbiel et al. 2008) and the models advanced in Pasko et al. (1999), Pasko and George (2002), Raizer et al. (2006, 2007, 2010) do not reflect related scenarios.

Krehbiel et al. (2008) discussed the charge imbalances in thunderstorms as a fundamental condition allowing propagation of leaders downward as cloud-to-ground lightning or upward as jet discharges. This demonstrated that upward discharges are analogous to cloud-to-ground lightning and providing a unified view on how lightning escapes from a thundercloud. Cummer et al. (2009) recently reported measurement of total charge of  $-144$  C transferred by a gigantic jet to the lower ionosphere, which is in the range of charge transfers to ground by strong negative cloud-to-ground discharges ( $-CGs$ ), however, associated with current rise time in gigantic jet ( $\sim 30$  ms), which is four orders of magnitude slower than in conventional  $-CGs$  ( $\sim 5$   $\mu s$ , Rakov and Uman 2003, pp. 7, 146, 154). Krehbiel et al. (2008) note that in accordance with existing experimental evidence the lightning initiation usually happens between adjacent charge regions of different polarity where the electric field is maximum. If the negative and positive charge centers are approximately equal in magnitude the bi-directional discharge propagates in the form of positive leaders inside of negative charge region and in the form of negative leaders inside of the positive charge region (e.g., Riousset et al. 2007). In this situation the leader system, which is assumed to be overall equipotential and neutral, remains at nearly zero potential (e.g., Riousset et al. 2007). Krehbiel et al. (2008) demonstrate that when the two charges are not balanced the leader potential can be significantly shifted in the direction defined by the charge with dominant magnitude and the propagation of the leader becomes essentially independent from the weaker charge center, allowing it to penetrate through the weaker charge center and to escape from the thundercloud. Krehbiel et al. (2008) presented a combination of observational and modeling results that indicate two principal ways in which upward discharges can be produced. The modeling presented in Krehbiel et al. (2008) indicates that blue jets occur as a result of electrical breakdown between the upper storm charge and screening charge attracted to the cloud top; they are predicted to occur 5–10 s or less after a cloud-to-ground or intracloud discharge produces a sudden charge imbalance in the storm. Gigantic jets are indicated to begin as a normal intracloud discharge between dominant mid-level charge and a screening-depleted upper level charge, that continues to propagate out the top of the storm (Krehbiel et al. 2008).

Figure 6 summarizes the results of simulating different types of discharges in normally electrified storms from Krehbiel et al. (2008). The lightning model employed to produce results shown in Fig. 6 uses a Lightning-Mapping-Array-Inferred multilayered charge structure positioned above a perfectly conducting flat ground plane (Riousset et al. 2007). The thundercloud and lightning discharge are modeled in a 3-D Cartesian domain using equidistant grids. The model uses a fractal approach to introduce stochasticity in a self-consistent model of the lightning channel, which fully satisfies Kasemir's hypothesis of equipotentiality and overall neutrality of the discharge (Kasemir 1960; Mazur and Ruhnke 1998; Riousset et al. 2007). In all cases shown in Fig. 6, the type of discharge results from a competition as to where breakdown is triggered first. Intracloud discharges usually win this competition because they occur between the two strongest charge regions during a storm's convective stages (Fig. 6a) (Krehbiel et al. 2008). The negative cloud-to-ground lightning discharges ( $-CGs$ , Figs. 6b, 6e) occur as descending precipitation generates lower positive charge (Williams 1989) or as the storm accumulates net negative charge, and can go either directly to ground or indirectly as a bolt-from-the-blue discharge (see discussion in Krehbiel et al. 2008). The negative gigantic jets ( $-GJs$ , Fig. 6f) provide an alternate way of relieving the mid-level negative charge, by discharging it to the upper atmosphere rather

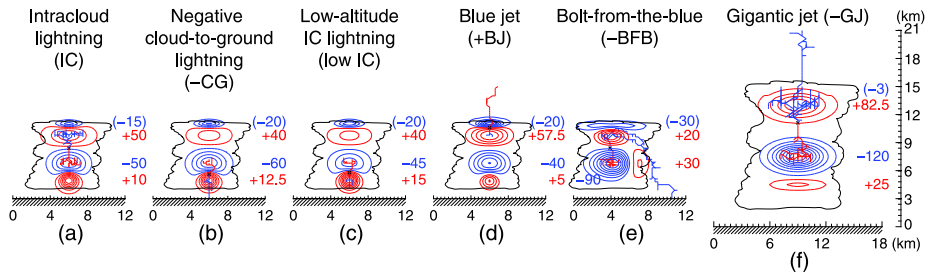


**Fig. 6** Simulated discharges illustrating the different known and postulated lightning types in a normally electrified storm (Krehbiel et al. 2008). (a–f), Blue and red contours and numbers indicate negative and positive charge regions and charge amounts (c), respectively, each assumed to have a Gaussian spatial distribution. A partially analogous set of discharges occurs or would be predicted to occur in storms having inverted electrical structures (see Fig. S5 in Krehbiel et al. (2008, Supplementary Information)). Reprinted from Krehbiel et al. (2008) by permission from *Nature Geoscience*

than to ground (Krehbiel et al. 2008). The positive blue jets (+BJs) do the opposite, namely transport positive charge upward (Fig. 6d; Krehbiel et al. 2008).

Recent confirmation of the theory advanced by Krehbiel et al. (2008) was provided by Lu et al. (2011b). These authors reported observations of two negative polarity gigantic jets. In both cases the gigantic jet producing flash began as ordinary intra-cloud lightning with upper level channels attempting to exit the cloud, and then produced the upward gigantic jet. Neither flash had developed channels to ground, confirming that the major charge transfer during gigantic jets occurred between the cloud and ionosphere (Lu et al. 2011b).

Recently Rioussset et al. (2010b) introduced a two-dimensional axisymmetric model of charge relaxation in the conducting atmosphere and applied this model in conjunction with three-dimensional lightning model proposed in Rioussset et al. (2007) to illustrate how blue and gigantic jet discharges are produced above cloud tops. The model reported by Rioussset et al. (2010b) accounts for the time dependent conduction currents and screening charges formed under the influence of the thundercloud charge sources and gives particular attention to realistic simulation of the dynamics of the screening charges near the cloud boundaries. The results demonstrate how the prior occurrence of intra-cloud discharges can prevent the development of a blue jet until a cloud-to-ground discharge enhances the excess of positive charge in the cloud by bringing negative charge to ground. The screening charge gradually developing at the cloud top leads to breakdown initiation near the cloud upper boundary, but is insufficient to contain the lightning leader channel within the cloud resulting in occurrence of upward propagating blue jet events. Furthermore, in thunderstorms where convective overturning near the cloud top is sufficiently strong, the screening layer that allowed for blue jet initiation, gets mixed with the storm's upper positive charge region, reducing the net positive charge in this region and causing a substantial charge imbalance between the two main layers of the thundercloud. Quantitative modeling of resulting discharge presented in Rioussset et al. (2010b) reveals that the leader channels cannot be contained in the volume enclosed within the cloud boundary and eventually escape upward to form a gigantic jet, consistent with the ideas first expressed by Krehbiel et al. (2008).

Results presented in Krehbiel et al. (2008), Rioussset et al. (2010b) provide experimentally substantiated mechanisms of escape of lightning leaders from cloud tops complementing the previous theoretical work (Petrov and Petrova 1999; Pasko et al. 1999; Pasko and George 2002; Tong et al. 2005; Raizer et al. 2006, 2007, 2010). The application of ideas advanced in Raizer et al. (2006, 2007, 2010) concerning possibility to map high poten-

tials at the cloud top to higher altitudes using conducting leaders depends on the possibility to sustain the leader process at low air pressures at high altitude. The understanding of the streamer-to-leader transition and the development of accurate numerical parameterizations of streamer zones of lightning leaders of different polarities, especially under low air pressure conditions, represent an important problem in current research on transient luminous events (e.g., Pasko 2006; Pasko and Bourdon 2007) and relevant recent work on this subject is reviewed in Sect. 5.2 below.

#### 4 Past, Present and Future Orbital Observation of TLEs

The first observation of a TLE from space was in a form of lightning associated emission layer at airglow altitude ( $\sim 95$  km) (Boeck et al. 1992), latter designated as elves (Fukunishi et al. 1996). The enhanced airglow events were recorded from space shuttle payload bay television cameras in a horizontal view. This first finding of lighting-induced airglow enhancement provided a new evidence of direct coupling between atmospheric lighting and enhanced airglow emission at the bottom of the ionosphere (Boeck et al. 1992). Elves, an acronym for Emission of Light and VLF perturbations due to EMP Source, were confirmed in ground observations using a multichannel high-speed photometer and image intensified CCD cameras at Yucca Ridge Field Station, Colorado as part of SPRITES'95 campaign in 1995 (Fukunishi et al. 1996).

During the STS-107 mission in January 2003, the Mediterranean Israeli Dust Experiment (MEIDEX) sprite campaign was conducted on board the space shuttle *Columbia* (Yair et al. 2003, 2004; Yair 2006). The total MEIDEX observation time was  $\sim 7$  hours. In  $\sim 51$  minutes of data collected over thunderstorms, 17 TLEs were identified including 7 sprites and 10 elves. The brightness of sprites was in the range of 0.3–1.7 MR in the 665 nm filter and 1.44–1.7 MR in the 860-nm filter. The estimated sprite detection rate was 0.13 sprites per minute (Yair et al. 2004). The observed elves were also analyzed, and the total emitted energy in the wavelength range 615–715 nm was estimated to be several to tens of kJ (Israelevich et al. 2004).

The LSO (Lightning and Sprite Observations) on board of ISS (International Space Station) is a first experiment dedicated to nadir observation of sprites in Earth orbit (Blanc et al. 2004, 2006, 2007). The first LSO measurements were conducted on the ISS in October of 2001. The LSO experiment used two digital space microcameras. One was equipped with a 762 nm narrowband filter targeting the specified  $1\text{PN}_2$  (3–1) band of sprites, and the other camera covered a visible wavelength range (400–1000 nm, with maximum sensitivity at 690 nm) targeting lightning and sprite emissions. The major challenge to observe TLEs in a nadir view was to identify sprite emissions in the presence of overlapping lightning emissions. Blanc et al. (2004, 2007) designed a novel technique to separate the sprite events from lightning. Specifically, the LSO experiment used a method of spectral differentiation between sprites and lightning based on sprite  $1\text{PN}_2$  (3–1) emission falling within the atmospheric absorption bands,  $\text{O}_2(b^1 \sum_g^+ - X^3 \sum_g^+)$  (0–0) around 761.9 nm, in which lightning emissions are significantly attenuated. The LSO was a pioneer experiment to prepare the TARANIS satellite mission. The nadir observation is necessary to simultaneously study the optical emissions, relativistic runaway electrons and associated X-ray and  $\gamma$ -ray emissions, that is one of the primary goals of the TARANIS mission (see further discussion below).

During 19 hours of the LSO observations, 40 events were registered, total 17 sprites, 3 halos and 9 superbolts. The sprite observation frequency was about 1.7 per hour (Blanc et al. 2006). The detection rate of sprites was 0.033 sprites per minute. In the respective observation areas of LSO, the Lightning Imaging Sensor (LIS) estimated the number of lightning



flashes to be about 1100 (Christian et al. 2003). Based on the fact that LSO observed only over the continents where 88% of the lightning occur, the occurrence of sprites number with respect to lightning was  $17 \times 88\% / 1100 = 1.4\%$ . Having considered that the global number of lightning determined from LIS observation was 44 flashes per second (Christian et al. 2003) or 2640 flashes per minute, the global occurrence rate of sprites was estimated to be  $2640 \times 1.4\% \sim 37$  sprites per minute (Blanc et al. 2006).

Present missions include ISUAL (2004) (Chern et al. 2003; Mende et al. 2006; Chen et al. 2008), Tatiana-1 (2005–2007) (Garipov et al. 2006), Tatiana-2 (2009) (Panasyuk et al. 2009; Garipov et al. 2010), and Sprite-Sat mission (2010) (Takahashi et al. 2006).

ISUAL (Imager of Sprites and Upper Atmospheric Lightnings) on board FORMOSAT-2 is the first satellite payload dedicated to the survey of the upper atmospheric discharge phenomena (Chern et al. 2003; Mende et al. 2006; Chen et al. 2008). The ISUAL project is an international collaboration between the National Cheng Kung University, Taiwan, Tohoku University, Japan and the instrument development team from the University of California, Berkeley. The ISUAL consists of three sensor packages including an intensified CCD imager, a six-channel spectrophotometer and a dual-band array photometer. The ISUAL observations have been successfully conducted during the first five years (2004–2009). Due to the significant scientific achievements during the first five years the ISUAL observations have been extended for three additional years (2010–2014) using funding from National Space Organization in Taiwan.

First sprite was recorded by ISUAL on July 4, 2004/21:31:15.451 (Mende et al. 2006). Furthermore, Mende et al. (2005) analyzed elves where the source lightning occurred beyond the solid Earth limb, and found that the elves contained significant 391.4 nm emission of the first negative  $N_2^+$  band system ( $1NN_2^+$ ). Mende et al. (2005) estimated that reduced electric field was  $> 200$  Td by comparing the ratio of ISUAL spectrophotometer measurements of TLE produced emissions to theoretically derived emission intensities. Using estimated reduced electric field and the measured and total ionization rates derived from  $1NN_2^+$  emission, an average electron density of  $210 \text{ electrons cm}^{-3}$  was estimated as being produced in the elves. Besides, the first FUV emissions (Lyman-Birge-Hopfield bands) were also detected in the ISUAL recorded elves (Mende et al. 2005). For sprites, Kuo et al. (2005) and Liu et al. (2006) estimated the intensities of electric field at the streamer tip to be  $2\text{--}4E_k$  using the ISUAL spectrophotometric measurements, while Adachi et al. (2006) analyzed ISUAL array photometer data and obtained the electric field of  $1\text{--}2E_k$  in the streamer region. As discussed in Sect. 3.2 the electric fields in sprite streamers are likely a factor of 1.5 higher (Celestin and Pasko 2010).

Chou et al. (2010) categorized ISUAL gigantic jets (GJs) into three types based on their generation dynamics and spectral properties. Type I GJs resemble those reported previously in Su et al. (2003), Kuo et al. (2009): after the fully developed jet (FDJ) established the discharge channel, the ISUAL photometers registered a peak that was from a return stroke-like-process. The associated ULF (ultra low frequency) spherics indicate that type I GJs are negative cloud-to-ionosphere discharges ( $-CIs$ ). Type II GJs begin as blue jets and then develop into GJs in  $\sim 100$  ms. Blue jets also frequently occurred in the same region before and after the type II GJs. No identifiable ULF spherics for the type II GJs were found, though an extra event reported in Chou et al. (2010) with  $+CI$  ULF was likely a type II GJ. Thus the energy and the charge in these events may not accumulate to high enough levels to initiate a bright gigantic jet. Type III GJs were preceded by a lightning, and a GJ occurred near this preceding lightning. The spectral data of the type III GJs are dominated by lightning signals and the ULF data have a high background noise. The average brightness of the type III GJs falls between those of the other two types of GJs. It was proposed that the discharge polarity

of the type III GJs could be either negative or positive, depending on the type of the charge imbalance left by the trigger lightning (Chou et al. 2010).

After analyzing the  $1\text{PN}_2$  brightness of the ISUAL elves and their FUV intensity and using modeling work for elves, Chang et al. (2010) demonstrated that ISUAL-FUV intensity of an elve could be used to estimate the peak current of the causative CG lightning. The ISUAL detection ratio of elves was improved since sensitivity of ISUAL FUV photometer is 16 times higher than that of ISUAL  $1\text{PN}_2$ -filtered Imager. Hence, FUV photometer can be used to perform survey of elves to infer the peak current of the elve-producing lightning and other salient parameters. Besides, existences of multielves, which are FUV events from the M-components or the multiple strokes in lightning flashes were also found. Lee et al. (2010) analyzed the distribution of the TLEs registered by ISUAL, and deduced the synoptic-scale factors that control the occurrence of TLEs. Two different distribution patterns were analyzed. For the low latitude tropical regions ( $25^\circ\text{S} \sim 25^\circ\text{N}$ ), 84% of the TLEs were found to occur over the Intertropical Convergence Zone (ITCZ) and the South Pacific Convergence Zone. The distribution of TLEs exhibited a seasonal variation that migrates North and South with respect to the equator. For the mid-latitude regions (latitudes beyond  $\pm 30^\circ$ ), 88% of the Northern winter TLEs and 72% of the Southern winter TLEs occurred near the mid-latitude cyclones. The winter TLE occurrence density and the storm track frequency share similar trends, with the distribution of the winter TLEs offset by  $10^\circ\text{--}15^\circ$ .

Tatiana-1 is a Moscow State University's research educational microsatellite. Measurements with this satellite were conducted during the period from January 2005 to March 2007 (Garipov et al. 2005b, 2005a, 2006). The instruments on board Tatiana-1 consisted of photomultiplier tubes (PMTs) for UV detection with wavelength band 300–400 nm and the detectors of extremely high-energy cosmic rays (EHECRs). The EHECRs were dedicated to observe Cherenkov atmospheric radiation, the secondary radiation characteristic of the electron passage through the atmosphere. Two years of UV data recorded by Tatiana-1 were analyzed, and the brightness (energy) and occurrence rate of UV events were compared with the lunar phase. The correlation between UV events and lunar phase was found. Moreover, the rate of UV flashes with energy release in the atmosphere greater than 50 kJ was four times higher at full moon night than at other moon phase (Garipov et al. 2008).

Shneider and Milikh (2010) studied the atmospheric electricity phenomena that could serve as a source for short millisecond range UV flashes. It was shown that UV flashes in the millisecond range detected by Tatiana-1 could be originating from gigantic blue jets (GBJ). The influence of an assumed self-consistent governing electric field in the GBJ streamer zone on the UV pulse shape and duration was revealed. It was also shown that red sprites can be a source for UV flashes with similar temporal profiles but at much lower intensity (Shneider and Milikh 2010).

Tatiana-2 satellite was launched on 17 September 2009 with a new set of instruments that includes UV (300–400 nm)- and red (600–700 nm)-filtered photomultiplier tube (PMT) micro-electro-mechanical telescope for extreme lighting (MTL), photo spectrometer and electron flux detector (Panasyuk et al. 2009; Garipov et al. 2010). The electron flux detector can detect the fluorescence light by penetrating electron with minimum energy greater than 1 MeV.

SPRITE-SAT is a micro satellite designed and developed by Tohoku University, Japan (Takahashi et al. 2006). The main scientific goal of SPRITE-SAT satellite is to simultaneously observe TLEs and terrestrial gamma-ray flashes (TGFs) in nadir direction and to study the relationship and generation mechanisms of TLEs and TGFs. The SPRITE-SAT has been successfully launched on January 23 2009 and operated by Tohoku University.

Future missions include Chibis-M (2010-) (Klimov et al. 2009), JEM-GLIMS (2011-) (Sato et al. 2009), ASIM (2014-) (Neubert et al. 2008), TARANIS (2016-) (Blanc et al. 2006; Lefeuve et al. 2009).

Chibis-M mission (Klimov et al. 2009) (see <http://chibis.cosmos.ru/>) is a micro-satellite mission designed for studies of TLEs and TGFs. In this mission, scientific instruments include X-ray and  $\gamma$ -ray detectors with energy range 50–500 keV and time resolution 30 ns, UV detector sensitive in wavelength range of 180–800 nm, digital photo camera with exposure time 0.2 second, radio frequency sensor with frequency range 20–50 Hz, and ULF-VLF antennas. Micro-satellite is to be delivered to ISS by a transport vehicle.

Global Lightning and sprItE MeasurementS on JEM-EF (JEM-GLIMS) is a space mission to observe lightning and TLEs from the Exposure Facility (EF) of the Japanese Experiment Module (JEM) at International Space Station (ISS) (Sato et al. 2009). The scientific goal of the JEM-GLIMS mission is to study the generation mechanism of TLEs and to identify the relationship between lightning, TLEs and TGFs (TGFs). The scientific instruments of the JEM-GLIMS mission consist of two CMOS cameras, two photometers, one spectro-imager, and two VHF receivers. JEM-GLIMS is dedicated to collaborate with the ground-based observations and with other space missions, such as TARANIS and ASIM (Sato et al. 2009).

ASIM (Atmosphere-Space Interactions Monitor) (Neubert 2009) is an instrument suite, mounted on an external platform of the European Columbus module for the International Space Station (ISS). The ASIM will be coordinated with ground EuroSprite campaigns (Neubert et al. 2008). The ASIM payload is equipped with Modular Multi-spectral Imaging Array (MMIA) and Modular X- and Gamma-ray Sensor (MXGS). The MMIA consist of cameras and photometers where cameras provide spatial resolution and photometers temporal resolution. The scientific goals of ASIM are (1) to find the source region of TLEs and TGFs, (2) to study the physics of TLEs and TGFs, (3) to study effects of water vapor and aerosols on cloud formation and atmospheric electricity, and (4) to capture meteor events (Neubert 2009).

TARANIS (Tool for the Analysis of Radiations from lightNings and Sprites) (Blanc et al. 2006; Lefeuve et al. 2009) is a CNES satellite project to study impulsive transfers of energy between the Earth atmosphere and the space environment. TARANIS will employ the micro-cameras, photometers, X-ray,  $\gamma$ -ray detectors, energetic electron detectors, and radio receiver and antenna. The goals of the mission are: (1) to advance the physical understanding of the links between TLEs and TGFs, (2) to clarify the potential signatures of impulsive transfers of energy, verified by physical mechanism, and (3) to characterize the physical parameters in TLEs and TGFs (Blanc et al. 2006; Lefeuve et al. 2009).

## 5 Chemical, Energetic and Electric Effects of TLEs on Local and Global Scales

### 5.1 Chemical Effects of TLEs

Atmospheric discharge phenomena (corona discharge, lightning and TLEs) are important sources of  $\text{NO}_x$  ( $\text{NO}$  and  $\text{NO}_2$ , summarized as  $\text{NO}_x$ ) in the troposphere and middle atmosphere.  $\text{NO}_x$  plays an important role in atmospheric chemistry since  $\text{NO}_x$  facilitates chemical reactions that influence the concentrations of ozone ( $\text{O}_3$ ) and hydroxyl radical ( $\text{OH}$ ) (Rakov and Uman 2003, p. 507). Appropriate quantification of lightning-produced  $\text{NO}_x$  and TLE-produced  $\text{NO}_x$  has become an important issue in studies of  $\text{NO}_x$  budget. The knowledge of occurrence rate and deposited energy, and understanding of triggered chemical reaction chain associated with lightning and TLEs are necessary to advance studies of  $\text{NO}_x$  budget.

However, the estimates of lightning induced  $\text{NO}_x$  ( $\text{LNO}_x$ ) vary by two orders of magnitude and range from 1 to 200  $\text{Tg(N) yr}^{-1}$ , where 1  $\text{Tg(N)} = 10^{12}$  grams of nitrogen. The estimates of TLEs induced  $\text{NO}_x$  ( $\text{TLE-NO}_x$ ) is limited because the types, occurrence rate and energy budget of TLEs are not well-studied (Rakov and Uman 2003, p. 508). The most recent accepted estimates of global  $\text{LNO}_x$  production range from 2 to 8  $\text{Tg(N) yr}^{-1}$  (Schumann and Huntrieser 2007). In other publications Cooray et al. (2009) used the knowledge on the electrical discharges to extrapolate the measurements of  $\text{NO}_x$  yield in laboratory spark experiments to that in lightning, and derived the global annual production of  $\text{NO}_x$  of about 4  $\text{Tg(N)}$ . Beirle et al. (2004) used Global Ozone Monitoring Instrument (GOME)  $\text{NO}_2$  column density and Lightning Imaging Sensor (LIS) to estimate 2.8  $\text{Tg(N) yr}^{-1}$ . Beirle et al. (2010) noted that uncertainty of  $\text{LNO}_x$  estimates might be biased due to a high variability of  $\text{NO}_2$  measurement for coincided lighting events and due to the fact that many  $\text{LNO}_x$  measurements are limited to the US region, not representative for global lighting.

Using in-situ  $\text{NO}_2$  measurements from the DC-8 aircraft missions and lightning data from National Lightning Detection Network, Bucsela et al. (2010) estimated the  $\text{LNO}_x$  production to be in the range of  $6\text{--}15 \times 10^{25}$  molecules per flash. To date, there are no direct measurements of TLE induced  $\text{NO}_x$  production. Peterson et al. (2009) estimated TLE- $\text{NO}_x$  production of blue jets and red sprites using the results of laboratory discharges. The blue jets were calculated to produce  $1.7 \times 10^{22}\text{--}7.4 \times 10^{26}$  molecules of  $\text{NO}_x$  per event while corresponding numbers for sprites were estimated to be  $6.8 \times 10^{23}\text{--}6.3 \times 10^{27}$  molecules of  $\text{NO}_x$  per event. On the basis of global TLEs occurrence rate (Ignaccolo et al. 2006), global annual  $\text{NO}_x$  production is estimated to be between  $7 \times 10^{23}\text{--}2 \times 10^{28}$  molecules per second (Peterson et al. 2009) with five order of magnitude uncertainty, corresponding to global TLE- $\text{NO}_x$  production of  $5.2 \times 10^{-4}$  to 14.7  $\text{Tg(N) yr}^{-1}$ . The above mentioned TLE- $\text{NO}_x$  estimates are still under debate (de Urquijo and Gordillo-Vazquez 2010; Nijdam et al. 2010; Peterson et al. 2010a, 2010b).

During the daytime, the  $\text{NO}_x$  gases are in photochemical balance in the stratosphere. After sunset  $\text{NO}$  is quickly converted to  $\text{NO}_2$  in reaction with  $\text{O}_3$ , and the nighttime  $\text{NO}_2$  measurements provide a good presentation of stratospheric  $\text{NO}_x$  (Arnone et al. 2008, 2009; Rodger et al. 2008). Arnone et al. (2008) investigated the  $\text{NO}_x$  production at sprite altitudes using the MIPAS (Michelson Interferometer for Passive Atmospheric Sounding) instrument on board European Space Agency's (ESA) ENViromental SATellite (ENVISAT). The ENVISAT is an advanced polar-orbiting Earth observation satellite launched by ESA, which provides measurements of the atmosphere, ocean, land, and ice [see also <http://envisat.esa.int>]. MIPAS is a limb-scanning Fourier Transform spectrometer recording emission spectra in the mid-infrared  $680\text{--}2410 \text{ cm}^{-1}$  ( $4.15\text{--}14.6 \mu\text{m}$ ) with spectral resolution of  $0.035 \text{ cm}^{-1}$ . The MIPAS scan across the horizon detecting atmospheric spectral radiances, which can be inverted to vertical temperature and trace species ( $\text{H}_2\text{O}$ ,  $\text{O}_3$ ,  $\text{CH}_4$ ,  $\text{N}_2\text{O}$ ,  $\text{HNO}_3$  and  $\text{NO}_2$  profiles) (Fischer et al. 2008). Arnone et al. (2008) adopted the Geo-fit Multi-Target Retrieval (GMTR) algorithm (Carlotti et al. 2006) to retrieve the two dimensional emission profile of  $\text{NO}_2$  from limb-scan data of MIPAS/GMTR on board of ENVISAT satellite. Arnone et al. (2008) used WWLLN (World Wide Lightning Location Network) lightning data as a proxy of sprite activity, and studied the possible sprite-induced  $\text{NO}_2$  perturbation, derived from MIPAS/GMTR data, over the region with intense WWLLN lightning activity during the period of August to December 2003.

Arnone et al. (2008) examined the mean nighttime WWLLN- $\text{NO}_2$  relationship at an altitude of 52 km, where MIPAS  $\text{NO}_2$  measurement coincided with high WWLLN lightning activity region, and suggested no significant impact on global scale of sprite perturbation for the time period August to December 2003. For a localized region measurements of

WWLLN-NO<sub>2</sub> in a 60-minute time window prior to MIPAS observations, the WWLLN-NO<sub>2</sub> data showed a positive displacement of about +1 ppbV (~10%) above the NO<sub>2</sub> background measurements ( $10 \pm 1.5$  ppbV). Arnone et al. (2008) indicated the possible observational evidence of ~10% NO<sub>2</sub> enhancement at sprite altitude of 52 km above the active thunderstorms, but provided no evidence of any significant increase on a global scale. Arnone et al. (2009) presented further analysis of an NO<sub>2</sub> enhancement as being dominated by the contribution from a region with low background winds north of the Equator (5°N to 20°N) during the first 30 to 40 days of the sample (i.e., the tail of Northern Hemisphere summer).

Rodger et al. (2008) inspected the possible sprite-induced nighttime NO<sub>x</sub> using GOMOS NO<sub>2</sub> measurements at altitudes of 20–70 km. The GOMOS (Global Ozone Monitoring by Occultation of Stars) on board ENVISAT satellite measures vertical profiles of minor gases using >600 occultations per day with global coverage. Rodger et al. (2008) selected four land/ocean regions from LIS/OTD five year lightning distribution data with strong regional and seasonal variations in lightning activities. The two to three orders of magnitude peak differences between lightning activity in the selected land/ocean regions were used to evaluate the corresponding variation of GOMOS nighttime NO<sub>2</sub> measurements at blue jet altitudes of 30–50 km and at sprite altitudes of 50–70 km. No significant variations coincided with lightning rate changes over land/ocean contrast, or seasonal variations shown in LIS/OTD distribution data. Rodger et al. (2008) concluded that TLE may cause local variations in NO<sub>x</sub>, but these do not appear to be significant on regional scales.

Huang et al. (2009) investigated the lightning-induced sudden brightening in the OH airglow layer using ISUAL 630-nm-filtered Imager. Huang et al. (2009) also proposed the conceptual mechanism of the induced OH nightglow enhancement. Huang et al. (2010) further analyzed 630-nm-filtered Imager recorded elves, and found that there is considerable intensity enhancement (~1.25 kR) unaccounted for after the N<sub>2</sub>1P contribution has been removed. Huang et al. (2010) suggested that there might be OH emissions in elves and that OH species might also be involved in the lightning-induced processes and contribute to the intensity enhancements that were observed.

Enell et al. (2008) studied the chemical effects of the electrical discharge phenomena in the middle atmosphere using an ion-neutral chemical model, also including the ionization, excitation, dissociation and chemical reactions of active species. The model considered the chemical production and loss with the electric discharge associated reactions and important ion-neutral chemical reactions. The reaction rates of the model were derived from Bolsig solver (Pitchford et al. 1981) and Siglo database [CPAT and Kinema Software]. Enell et al. (2008) used the derived  $E$ -field ( $\sim 0.5$ – $2E_k$ ) from ISUAL recorded TLE events at altitudes of 53, 63, 73, 83 km (Adachi et al. 2006) as input electric fields in the model. The modeling results show that the NO<sub>x</sub> enhancements are at most one order of magnitude in the streamers, corresponding to at most 10 mol per event. Given the estimated global occurrence rate (3 per minute), the global production of NO<sub>x</sub> by sprites is 150–1500 kg/day, i.e.,  $5.5 \times 10^{-5}$ – $5.5 \times 10^{-4}$  Tg(N).

Sentman et al. (2008) utilized a simplified sprite streamer model coupled with the full kinetic modeling including 80+ species and 800+ chemical reactions. The species in their comprehensive kinetic model included background neutrals and atoms and their different electronic states, negative/positive ions and ion clusters. The reaction set considered the reactions accounting for cosmic ray background, electric field driven electron impact processes, electron-ion recombination, attachment-detachment processes, ground/active state chemistry, collisional and radiative deactivation, ion conversion and ion-ion recombination, odd hydrogen/nitrogen reactions, and positive/negative ion/chlorine chemistry. The sprite streamer model at an altitude of 70 km (Sentman et al. 2008) utilized an impulsive electric

field at the streamer tip. The electric field was modeled as  $E_h(t) = E_0 e^{-(t-t_0)^2/\Delta t^2}$  where  $E_0 = 5E_k$ , five times of the magnitude of breakdown electric field  $E_k$ , and  $\Delta t$  is the characteristic time duration (6  $\mu$ s) of the impulse centered at time  $t_0$ . In the streamer head, the modeled impulse electric field triggered a series of chemical reaction chains. The principal chemical reactions were electron impact processes at streamer tip. The produced active chemical species remained in the trailing column of the streamer, and the chemiluminescent emissions persisted in that afterglow region for the time duration greater than tens of seconds (Sentman et al. 2008).

The simulation results of Sentman et al. (2008) predicted that the weak ( $\sim 1$  kR), but possibly detectable, OI 557.7 nm and O<sub>2</sub> atmospheric airglow emissions and OH Meinel emissions ( $\sim 1$ –10 R). The derived sprite parameters (emission rate and brightness) in the plasma chemistry streamer model were consistent with ground observation of sprites (Stenbaek-Nielsen and McHarg 2008). Sentman and Stenbaek-Nielsen (2009) simulated the streamer plasma chemistry accounting for non-zero field ( $< 0.5E_k$ ) in the trailing region of the streamer channel. The results showed that the electron densities in the trailing region were slightly reduced due to enhanced dissociative attachment in the undervoltage environment. The densities of O(<sup>3</sup>P) and the metastable species O(<sup>1</sup>D) and N<sub>2</sub>(A<sup>3</sup> $\Sigma_u^+$ ) were enhanced by a modest factor of 2 or less compared with a field-free tail. The O<sub>2</sub>(a<sup>1</sup> $\Delta_g$ ) species showed slightly greater enhancements, by up to a factor of 3, and O showed enhancements by up to a factor of 5.

Gordillo-Vazquez (2008) developed a full time-dependent kinetic model to consider the microscopic collisional and radiative processes underlying the optical flashes associated with an impulsive discharge in the single sprite streamer passing through the air region in the mesosphere at altitudes, 63, 68 and 78 km. The kinetic model for air plasma included more than 75 species and almost 500 reactions. The reaction set in the kinetic model took into account the possible impact of H<sub>2</sub>O (humid chemistry). The modeling results predicted the radiative emissions associated with vibrational kinetics of N<sub>2</sub> and CO<sub>2</sub>, and local enhancement of NO<sub>x</sub> at different altitudes. All calculations were conducted for midnight conditions in mid-latitude regions (+38N°) and 0° latitude. The initial values of the neutral species were taken from the Whole Atmosphere Community Climate Model (WACCM). The kinetic model of Gordillo-Vazquez (2008) assumed that a sprite streamer had a step-like impulse electric field with a peak value of  $3.3E_k$  and time duration 5  $\mu$ s in the streamer head, and weak electric field in the afterglow region in the streamer body. The characteristic value of electric field in the streamer body was 1 Td. The results demonstrated that the impact of 4 ppm of H<sub>2</sub>O was only slightly visible in O<sub>3</sub><sup>−</sup> at 68 and 78 km while it strongly affected the behavior of the anion CO<sub>4</sub><sup>−</sup> at all the altitudes investigated. At 68 km, the concentrations of NO and NO<sub>2</sub> increased by about one order of magnitude while that of NO<sub>3</sub> exhibited a remarkable growth of up to almost three orders of magnitude. Gordillo-Vazquez (2008) investigated the brightness of the radiative transitions associated with sprite in the visible, IR and UV band emissions. The reported brightness of LBH band was always higher than the NO- $\gamma$  band system. The vibrationally excited CO<sub>2</sub> emission bands (4.26, 9.4, 13.9 and 14.9  $\mu$ m) exhibited noticeable enhancements of radiative emissions.

Liu and Pasko (2007) developed a model to study NO- $\gamma$  emissions ( $\text{NO}(\text{A}^2\Sigma^+) \rightarrow \text{NO}(\text{X}^2\Pi) + h\nu$ ) associated with streamer discharges in air at different pressures. The modeling results indicate that the  $\text{NO}(\text{A}^2\Sigma^+)$  species in sprite streamers at 70 km altitude are mostly produced by interaction of N<sub>2</sub>(A<sup>3</sup> $\Sigma_u^+$ ) metastable species with high-density ambient  $\text{NO}(\text{X}^2\Pi_r)$ , molecules via reaction  $\text{N}_2(\text{A}^3\Sigma_u^+, w) + \text{NO}(\text{X}^2\Pi_r, v) \rightarrow \text{NO}(\text{A}^2\Sigma^+, v') + \text{N}_2(\text{X}^1\Sigma_g^+, w')$ . Analysis of the production and loss mechanisms for the upper excited states leading to NO- $\gamma$  and N<sub>2</sub> Lyman-Birge-Hopfield (LBH) emissions demonstrates that the total



intensity of NO- $\gamma$  emissions associated with sprites is substantially weaker than that of the N<sub>2</sub> LBH emissions. Campbell et al. (2007) recently emphasized importance of N<sub>2</sub>(A<sup>3</sup> $\Sigma_u^+$ ) + O  $\rightarrow$  NO + N(<sup>2</sup>D) reaction for production of NO in the upper atmosphere. Gordillo-Vazquez (2008) indicated possible importance of the direct electron impact excitation of NO(A<sup>2</sup> $\Sigma^+$ ) in sprite discharges as source of NO- $\gamma$  emissions. The significance of the direct excitation is determined by the cross section of the related process, which varies by two orders of magnitude in the available literature (see Gordillo-Vazquez 2008, and references therein). Liu and Pasko (2010) have recently reviewed publications with relevant experimental data, and utilized streamer modeling to conclude that the direct electron impact excitation is not the dominant production mechanism for NO(A<sup>2</sup> $\Sigma^+$ ) species.

Analysis of ISUAL spectrophotometric data in the context of sprite streamer modeling has been reported in Liu et al. (2009b). These authors simulated two positive model streamers developing in strong and weak applied electric fields (with respect to  $E_k$ ) at 70 km latitude. The intensity ratio of the second positive band system of N<sub>2</sub> to the first negative system of N<sub>2</sub><sup>+</sup> was obtained separately from the modeling and the ISUAL measurements. The comparison results indicate that the ratio obtained for the streamer developing in an electric field close to the conventional breakdown threshold field  $E_k$  agrees with the ISUAL measurements at the very early stage of the sprite development better than for the streamer developing in a field much lower than  $E_k$ . The authors utilized the strong field streamer case in conjunction with the ISUAL data to gain additional information on the poorly known quenching altitude of the N<sub>2</sub>(a<sup>1</sup> $\Pi_g$ ) state, which is responsible for N<sub>2</sub> LBH band system. The results supported the conclusions of the previous study by Liu and Pasko (2005) that the 77 km is a good estimate for the quenching altitude of N<sub>2</sub>(a<sup>1</sup> $\Pi_g$ ).

Gordillo-Vazquez and Donko (2009) considered the effect of relative humidity on plasma chemistry model. The relative humidity of the atmospheric air between 0 and 15 km can change between 15% and 100% depending on the altitude investigated and the ambient temperature. The reported calculations suggested that the relative humidity had a clear impact on the behavior of the electron energy distribution function (EEDF) and magnitude of the transport coefficients of air plasmas at ground (0 km) and room temperature conditions (293 K). At higher altitudes (11 and 15 km), the influence of the relative humidity was negligible when the values of the gas temperature were assumed to be the 'natural' ones corresponding to those altitudes, that is,  $\sim 215$  K (at 11 km) and  $\sim 198$  K (at 15 km). However, it was found that a small enhancement (of maximum 100 K) in the background gas temperature (that could be reasonably associated with the TLE activity) would lead to a remarkable impact of the relative humidity on the EEDF and transport coefficients of air plasmas under the conditions of blue jets, blue starters and gigantic jets at 11 and 15 km. The latter effects were visible for relatively low reduced electric fields ( $E/N > 25$  Td) that could be controlling the afterglow kinetics of the air plasmas generated by TLEs.

Recently, Hiraki et al. (2008) and Hiraki (2009) used an ion-neutral chemical model to calculate the chemical effects under two situations. The first one corresponded to the impulsive electric field case. Hiraki et al. (2008) assumed a streamer tip with an impulsive electric field in the discharge region of TLEs. The tip region had a uniform magnitude of electric field (150 kV/cm) and moved at streamer speed  $\sim 10^7$  cm/s. Nighttime condition results demonstrated that the densities of NO, O<sub>3</sub>, H, and OH increased suddenly through reactions triggered by the initial atomic nitrogen and oxygen products and electrons just after streamer initiation. The NO and NO<sub>2</sub> species still remained for 1 hour, predominantly around an altitude of 60 km. Other species (O<sub>3</sub>, OH, HO<sub>2</sub> and H<sub>2</sub>O<sub>2</sub>) remained in the altitude range between 40 and 70 km. The second considered situation corresponded to the quasi-electrostatic case. Hiraki (2009) calculated the chemical perturbations due to the lightning-induced electric field. Hiraki (2009) found that the recovery timescale of the electron density

was much longer than the interval of the lightning stroke ( $\sim 10$  ms). The subsequent sprite events as well as the related field dynamics could be well affected by the residual effects of the primary sprite event (Hiraki 2009).

Haldoupis et al. (2010) reported narrowband VLF observations in which multiple transmitter-receiver VLF pairs with great circle paths passing near a sprite-producing thunderstorm were available, and presented an evidence that visible sprite occurrences are accompanied by early VLF perturbations in a one-to-one correspondence. The early VLF events are abrupt perturbations of sub-ionospherically propagating VLF waves (including both perturbations in amplitude and phase) that occur within 20 ms of a lightning event. These events have been discussed in Sect. 3.1 of this review with relationship to elves. The observations of Haldoupis et al. (2010) imply that the sprite generation mechanism may cause also sub-ionospheric conductivity disturbances that produce early VLF events. However, the one-to-one visible sprite to early VLF event correspondence, if viewed conversely, appears not to be always reciprocal (Haldoupis et al. 2010). This is because the number of early events detected in some case studies was considerably larger than the number of visible sprites. Since the great majority of the early events not accompanied by visible sprites appeared to be caused by positive cloud to ground (+CG) lightning discharges, it is possible that sprites or sprite halos were concurrently present in these events as well but were missed by the sprite-watch camera detection system (Haldoupis et al. 2010). In terms of general discussion of conductivity/chemical perturbations associated with sprites the average conductivity in sprite volume deduced from ELF radiation emitted by sprite current is  $\sim 10^{-7}$  S/m (Pasko et al. 1998b). A recent study of Gordillo-Vazquez and Luque (2010) indicates that larger conductivity changes are possible due to associative detachment of electrons from  $O^-$  ions in the trailing regions of long sprite streamers when electric field in these regions approaches the conventional breakdown threshold field during the later stages of sprite evolution (Liu 2010; Luque and Ebert 2010).

## 5.2 Energetic Effects of TLEs

TLEs are discharge phenomenon, representing the mechanism for energy transfer from the tropospheric charge separation and lightning to the middle atmosphere and the ionosphere. The physical mechanism of TLEs is similar to charge/discharge or dielectric breakdown in a capacitor between two conducting planes. The redistribution of charge in the thunderstorm can generate strong electrostatic fields at high altitudes and the current in a lightning stroke can radiate the electromagnetic field. The leader process in lightning channels may produce runaway electrons leading to X-ray and gamma-ray emissions. The interactions between electric fields and particles in the middle atmosphere cause energy pooling or air breakdown in large volumes between the ground and the bottom of ionosphere. The transferred energy is released in the form of radiated photons (UV, visible, infrared emissions, X-rays and gamma-rays), stored in the medium in the form of vibrationally or electronically excited metastable species, or deposited as heat, leading to generation of infrasound waves. Review of recent literature relevant to infrasound emissions and heating effects of TLEs is included below in this subsection.

The global occurrence rates of TLEs are important to understand in order to estimate their effects on  $NO_x$  budget and energy budget in the mesosphere. First such estimations were conducted using ELF emissions from lightning discharges during a time period between June 19, 2001 and January 20, 2002. Based on the empirical sprite initiation probability with critical charge moment change, the global occurrence rate of sprites was estimated

to be 0.5 sprites per minute (Sato and Fukunishi 2003). In MEIDEX mission, the average detection rate of TLEs during the MEIDEX was 0.13 sprites per minute (Yair et al. 2004). Multiplying the detection rate of sprites (0.13) by a conservative estimate of simultaneous tropical thunderstorms (100), we get a global occurrence rate of 13 sprites per minute in the tropics. In LSO mission, the detection rate of sprites was 0.3 sprites per minute and estimated global occurrence rate of sprites was  $\sim 37$  sprites per minute (Blanc et al. 2004). Using ground observations, (Ignaccolo et al. 2006) estimated the occurrence rate of sprites to be  $\sim 2.8$  events per minute. Chen et al. (2008) and Hsu et al. (2009) analyzed ISUAL data during an extended time period from 2004 to 2009 and reported the occurrence rate of TLEs of different types: 72, 3.7 and 1 per minute for elves, halos and sprites, respectively. The average observed  $1\text{PN}_2$  energies in elves, halos and sprites are 1.9, 1.4 and 2.2 MJ, respectively (Kuo et al. 2008). Having considered the ratio of  $1\text{PN}_2$  excitation rate to the total collision rates for the electron impact processes in the 78.1%  $\text{N}_2$  and 20.9%  $\text{O}_2$  air mixture, the ratio of total energy deposition to the  $1\text{PN}_2$  energy is about 10. Therefore, the average energy deposition of elves, halos and sprites are 19, 14 and 22 MJ, respectively (Kuo et al. 2008). Therefore, elves, halos and sprites deposit 1370, 52 and 22 MJ of tropospheric energy in the middle atmosphere (Hsu et al. 2009).

In comparison to a typical total energy of 1–10 GJ in the cloud-to-ground (CG) lightning, the average total energy deposition (22 MJ) per sprite estimated by Kuo et al. (2008) is consistent with the theoretical calculation 1–10 MJ by Sentman et al. (2003). Other work based on scaling of observed optical emission line ratios had suggested that the total energy deposited in the mesosphere by sprites could be as large as 1 GJ (Heavner et al. 2000). Using infrasound detection with a method independent of an optical measurement, Farges et al. (2005) estimated a range of total energy between 0.4 and 40 GJ. Recently, Takahashi et al. (2010) estimated the optical energy of sprites using ISUAL array photometer. The averages of the time-integrated optical energies are 176 kJ and 119 kJ for the  $1\text{PN}_2$  and second positive  $\text{N}_2$  ( $2\text{PN}_2$ ) band systems, respectively (Takahashi et al. 2010). Hence, the presently estimated total energy deposition by sprites varies by many orders of magnitude (1 MJ to 40 GJ) and depends on particular measurement technique employed. Both, the global occurrence rates of different types of TLEs and their energy budget are still poorly quantified and require further investigation.

Farges and Blanc (2010) reported inverted-chirp infrasonic signals with high frequencies arriving before low frequencies, possibly emitted by sprite discharges and observed on the ground at close range ( $< 100$  km) from the source. Following this report de Larquier and Pasko (2010) utilized a parallel version of a two-dimensional finite-difference time-domain model of infrasound propagation in a realistic atmosphere to demonstrate that the observed morphology of infrasound signals is consistent with general scaling of diameters of sprite streamers inversely proportionally to the air density. The smaller structures at lower altitudes radiate higher infrasonic frequencies that arrive first at the observational point on the ground, while the low frequency components are delayed because they originate at lower air densities at higher altitudes. Results of Farges and Blanc (2010) suggest that the observed infrasound signal is strongly related to the sprite vertical extent. The absorption of infrasonic waves increases with altitude and is generally proportional to the square of frequency (e.g., Sutherland and Bass 2004; de Groot-Hedlin 2008). Therefore the absorption scaling through the sprite vertical extent may be at least partly responsible for the observed infrasonic signal. Specifically, it was noted by de Larquier and Pasko (2010) that the signal arriving from higher altitudes would naturally have a depleted high frequency content. Also, geometrical considerations indicate that such a signal would arrive to an observer positioned several tens of kilometers horizontal distance from the sprite with some delay with respect to the signal emitted from the lower portions of the sprite. The quantitative results of de Larquier and

Pasko (2010) demonstrate that strong absorption of high frequency infrasonic components at high altitudes (i.e., similar to 0.2 dB/km for 8 Hz at 70 km) may also contribute to formation of inverted-chirp signals observed on the ground at close range.

The general scaling of the Joule heating time scale in the streamer channels as a function of air density can be quite easily deduced from basic similarity analysis of gas discharges to be inversely proportional to square of gas density (e.g., Achat et al. 1992; Tardiveau et al. 2001; Pasko 2006). Therefore it is generally expected that the heating processes and resulting streamer-to-leader transition should be delayed with reduction of air pressure (i.e., at higher altitudes in the Earth atmosphere) and it should be possible to define a set of specific conditions (i.e., altitude range, reduced electric field  $E/N$ , etc.) in the Earth atmosphere for which the transition becomes impossible. The visual appearance of some blue jets and gigantic jets [see for example Fig. 2 in Pasko et al. (2002), Fig. 1 in Wescott et al. (2001) and Fig. 10 in Pasko and George (2002)] is suggestive of a transition from hot lightning like channels to a cold streamer dominated region at higher altitudes. In terms of negative leader phenomenology, the moment of attachment of gigantic jet to the lower ionospheric boundary, can be interpreted as the “final jump stage”, when the leader streamer zone makes contact with the opposite electrode (Bazelyan and Raizer 1998, p. 212). This stage may also have some resemblance to the negative corona flash stage of negative leader development (Bazelyan and Raizer 2000, p. 199). The high speeds during the final jump,  $5 \times 10^4$  m/s to  $10^6$  m/s (Bazelyan and Raizer 1998, p. 212), are consistent with the range of speeds, from  $5 \times 10^4$  m/s to more than  $2 \times 10^6$  m/s, reported in Pasko et al. (2002). Kuo et al. (2009) recently reported first photometric measurements of the fast  $\sim 10^7$  m/s upward propagation during the initial stage (also referred to as fully developed stage in Su et al. 2003) of a gigantic jet probably indicating highly overvolted conditions, which streamers experienced as they moved to low air density (high reduced electric field  $E/N$ ) regions at high altitude. The relatively bright persistent channel below  $\sim 40$ – $50$  km altitude observed in gigantic jets (Pasko et al. 2002; Su et al. 2003) and designated as trailing jet in Su et al. (2003), can be interpreted as an attempt of the negative leader to form a next step, which has not succeeded (possibly due to a fast dielectric relaxation response of a conducting atmosphere or a significant lengthening of the heating time scales at low air pressures).

As discussed recently in Rioussset et al. (2010a, see also extensive list of references cited therein) there are two principal approaches that are used in the existing literature for modeling studies of air heating effects in streamer discharges. The first one usually postulates either a time-dependent or a stationary current and derives time dynamics of the electric field, conductivity and other parameters of the channel assuming continuity of the current along the channel. The second approach assumes a constant value of the electric field in the channel and then self-consistently evaluates dynamics of other discharge parameters (i.e., conductivity, current, gas temperature, etc.). The second approach describes very well a situation after the streamer bridges a relatively short gap with a constant applied voltage, and there are several related experiments conducted under controlled laboratory conditions at ground and near ground air pressures in which streamer-to-spark transition times have been accurately measured (e.g., Černák et al. 1995; Larsson 1998). Rioussset et al. (2010a) have recently reported modeling results relevant to the second approach. The related model set up represents a first step toward development of more general and scalable with air density leader models, and is motivated by the possibility to carefully test the model calculated streamer-to-spark transition times in comparison with experimental data. Rioussset et al. (2010a), in particular, presented a formulation of streamer-to-spark transition model that allowed studies of gas dynamics and chemical kinetics involved in heating of air in streamer channels for a given air density  $N$  under assumption

of constant applied electric field  $E$ . The model accounts for the dynamic expansion of the heated air in the streamer channel and resultant effects of  $E/N$  variations on plasma kinetics, the vibrational excitation of nitrogen molecules  $N_2(v)$ , effects of gains in electron energy in collisions with  $N_2(v)$ , and associative ionization processes involving  $N_2(A^3\Sigma_u^+)$  and  $N_2(a'^1\Sigma_u^-)$  species. The results are in excellent agreement with available experimental data at ground and near ground air pressures, and demonstrate that for the air densities corresponding to 0–70 km altitudes the kinetic effects lead to a significant acceleration of the heating, with effective heating times scaling closer to  $1/N$  than to  $1/N^2$  predicted on the basis of similarity laws for Joule heating (Riousset et al. 2010a). This acceleration is attributed to a strong reduction in electron losses due to three-body attachment and electron–ion recombination processes with reduction of air pressure (Riousset et al. 2010a).

### 5.3 Global Electric Circuit Effects of TLEs

As part of this review we also make some remarks as to recent research on global electric circuit processes as relevant to TLEs. It is well understood that electrified shower clouds, thunderstorms and lightning provide contributions to the total generator current in the global electric circuit with well defined, and also relatively well understood diurnal and annual variability (e.g., Mareev et al. 2008; Mareev 2010; Williams 2009; Liu et al. 2010, and references therein). Recent research indicates that in addition to above mentioned components there are several other types of electrical processes that may contribute to the global electric circuit (these include both charging and discharging effects). In particular, modeling studies reported in Krehbiel et al. (2008) emphasize that the recently discovered transient luminous events called gigantic jets (Pasko and Stenbaek-Nielsen 2002; Su et al. 2003) are highly energetic discharges forming a direct electrical path for transferring main negative charge of a thundercloud to the lower ionosphere (discharging the global electric circuit). These events are developing on time scales measured in hundreds of milliseconds. The charge transfers have only recently been measured and can exceed 100 C in one event (for example 144 C were reported in Cummer et al. 2009). Also, it is now known that sprite type of transient luminous events is driven by cloud-to-ground lightning discharges that possess significant continuing current. These discharges can move hundreds of Coulombs of positive charge to ground on a time scale of hundreds of ms. Cummer and Fullekrug (2001) reported an example of such discharge in which 850 C of charge were transferred in 150 ms. Given approximately 200,000 C residing in the global electric circuit, this indicates that on the order of 0.1% of that total can be moved in a single event. Although these events do not occur often (Williams 2009), their transient effects can be measurable (Fullekrug and Rycroft 2006; Rycroft and Odzimek 2010). Rycroft and Odzimek (2010) summarize recent parameterizations that are used to model thunderclouds and discuss an engineering model of global electric circuit including transient aspects related to lightning and sprites. This model is one of few current models that treats transient global electric circuit solutions. Rycroft and Odzimek (2010) point, in particular, that the role of high altitude intra-cloud lightning discharges is not fully understood and requires further investigation.

## 6 Summary and Concluding Remarks

In this review article we introduced transient luminous events of different types, including elves, sprite halos, sprites, blue jets and gigantic jets. Then, we described phenomenological features of sprites, including meteorological conditions leading to their production, parent

lightning parameters, and their shapes, sizes, and dynamical characteristics of their formation. The most recent advances in modeling of elves have been presented, including event based finite-difference time-domain modeling allowing direct comparison with satellite observations. The review of theory on sprites and sprite halos focused on most recent literature devoted to initiation of sprite streamers, their observed exponential expansion, and their electrical connection to the lower ionosphere. A recently proposed view of mechanisms of blue and gigantic jets has been presented that emphasizes charge imbalances in thunderstorms and analogies with conventional cloud to ground discharges to articulate conditions leading to upward escape of lightning leaders and their propagation toward the ionosphere. We then reviewed various local and global effects of TLEs. In this context existing and planned orbital observations have been discussed in detail. That discussion followed by presentation of the summary of the most recent literature on chemical, energetic and global electric circuit effects of TLEs.

There are many experimental as well as theoretical problems that remain to be solved in TLE studies. Examples in theoretical field include exact mechanisms of initiation and propagation of sprite streamers in low applied electric fields, role of thermal electron runaway phenomena in lightning and different types of TLEs, and development of self-consistent quantitative theory of transition of electrical discharge from thermal (leader dominated) forms at low altitudes to non-thermal (streamer dominated) forms at lower air densities at high altitudes in the Earth's atmosphere (e.g. Pasko 2006, and references therein). Examples in experimental field include a definite need for higher resolution spectral measurements of rotational intensity distributions of  $N_2$  molecular bands that would allow accurate determination of rotational temperatures in sprites (e.g. Pasko 2007, and references therein), and a definite need for at least 100 times better time resolution to resolve many missing details in blue and gigantic jets (e.g. Pasko 2010, and references therein).

**Acknowledgement** Participation of V.P. Pasko was supported by the United States National Science Foundation under AGS-0734083 and AGS-0836391 grants to Penn State University.

## References

- S. Achat, Y. Teisseyre, E. Marode, The scaling of the streamer-to-arc transition in a positive point-to-plane gap with pressure. *J. Phys. D, Appl. Phys.* **25**(4), 661–668 (1992)
- T. Adachi, H. Fukunishi, Y. Takahashi, M. Sato, Roles of the EMP and QE field in the generation of columniform sprites. *Geophys. Res. Lett.* **31**(4), L04107 (2004). doi:[10.1029/2003GL019081](https://doi.org/10.1029/2003GL019081)
- T. Adachi, H. Fukunishi, Y. Takahashi, Y. Hiraki, R.R. Hsu, H.T. Su, A.B. Chen, S.B. Mende, H.U. Frey, L.C. Lee, Electric field transition between the diffuse and streamer regions of sprites estimated from ISUAL/array photometer measurements. *Geophys. Res. Lett.* **33**(17), L17803 (2006)
- T. Adachi, Y. Hiraki, K. Yamamoto, Y. Takahashi, H. Fukunishi, R.R. Hsu, H.T. Su, A.B. Chen, S.B. Mende, H.U. Frey, L.C. Lee, Electric fields and electron energies in sprites and temporal evolutions of lightning charge moment measurements. *J. Phys. D, Appl. Phys.* **41**(23), 234010 (2008)
- E. Arnone, A. Kero, B.M. Dinelli, C.F. Enell, N.F. Arnold, E. Papandera, C.J. Rodger, M. Carlotti, M. Ridolfi, E. Turunen, Seeking sprite-induced signatures in remotely sensed middle atmosphere  $NO_2$ . *Geophys. Res. Lett.* **35**, L05807 (2008)
- E. Arnone, A. Kero, C.F. Enell, M. Carlotti, C.J. Rodger, E. Papandera, N.F. Arnold, B.M. Dinelli, M. Ridolfi, E. Turunen, Seeking sprite-induced signatures in remotely sensed middle atmosphere  $NO_2$ : latitude and time variations. *Plasma Sources Sci. Technol.* **18**, 034014 (2009)
- T. Asano, M. Hayakawa, M. Cho, T. Suzuki, Computer simulations on the initiation and morphological difference of Japan winter and summer sprites. *J. Geophys. Res.* **113**(A2), A02308 (2008). doi:[10.1029/2007JA012528](https://doi.org/10.1029/2007JA012528)
- T. Asano, T. Suzuki, M. Hayakawa, M.G. Cho, Three-dimensional EM computer simulation on sprite initiation above a horizontal lightning discharge. *J. Atmos. Sol.-Terr. Phys.* **71**, 983–990 (2009a)



- T. Asano, T. Suzuki, Y. Hiraki, E. Mareev, M.G. Cho, M. Hayakawa, Computer simulations on sprite initiation for realistic lightning models with higher-frequency surges. *J. Geophys. Res.* **114**, A02310 (2009b)
- C.P. Barrington-Leigh, U.S. Inan, M. Stanley, Identification of sprites and elves with intensified video and broadband array photometry. *J. Geophys. Res.* **106**(A2), 1741–1750 (2001). doi:[10.1029/2000JA000073](https://doi.org/10.1029/2000JA000073)
- E.M. Bazelyan, Y.P. Raizer, *Spark Discharge* (Chemical Rubber Company Press, New York, 1998)
- E.M. Bazelyan, Y.P. Raizer, *Lightning Physics and Lightning Protection* (IoP Publishing, Bristol, 2000)
- S. Beirle, U. Platt, M. Wenig, T. Wagner, NO<sub>x</sub> production by lightning estimated with GOME. *Adv. Space Res.* **34**(4) Sp. Iss., 793–797 (2004). doi:[10.1016/j.asr.2003.07.069](https://doi.org/10.1016/j.asr.2003.07.069)
- S. Beirle, H. Huntrieser, T. Wagner, Direct satellite observation of lightning-produced NO<sub>x</sub>. *Atmos. Chem. Phys.* **10**(22), 10965–10986 (2010). doi:[10.5194/acp-10-10965-2010](https://doi.org/10.5194/acp-10-10965-2010)
- E. Blanc, T. Farges, R. Roche, D. Brebion, T. Hua, A. Labarthe, V. Melnikov, Nadir observations of sprites from the international space station. *J. Geophys. Res.* **109**(A2), A02306 (2004). doi:[10.1029/2003JA009972](https://doi.org/10.1029/2003JA009972)
- E. Blanc, T. Farges, D. Brebion, A. Labarthe, V. Melnikov, Observations of sprites from space at the nadir: the LSO (lightning and sprite observations) experiment on board of the international space station, in *Sprites, Elves and Intense Lightning Discharges*, ed. by M. Füllekrug, E.A. Mareev, M.J. Rycroft. NATO Science Series II: Mathematics, Physics and Chemistry, vol. 225 (Springer, Heidelberg, 2006), pp. 151–166
- E. Blanc, T. Farges, A.N. Belyaev, V.V. Alpatov, D. Brebion, A. Labarthe, V. Melnikov, Main results of LSO (Lightning and Sprite Observations) on board of the International Space Station. *Microgravity Sci. Technol.* **19**(5–6), 80–84 (2007)
- W.L. Boeck, O.H. Vaughan, R.J. Blakeslee, B. Vonnegut, M. Brook, Lightning induced brightening in the airglow layer. *Geophys. Res. Lett.* **19**, 99–102 (1992)
- W.L. Boeck, O.H. Vaughan, R.J. Blakeslee, B. Vonnegut, M. Brook, J. McKune, Observations of lightning in the stratosphere. *J. Geophys. Res.* **100**, 1465–1475 (1995)
- W.L. Boeck, O.H. Vaughan, R.J. Blakeslee, B. Vonnegut, M. Brook, The role of the space shuttle videotapes in the discovery of sprites, jets and elves. *J. Atmos. Sol.-Terr. Phys.* **60**, 669–677 (1998)
- E. Bucsela, J. Morrill, M. Heavner, C. Siefring, S. Berg, D. Hampton, D. Moudry, E. Wescott, D. Sentman, N<sub>2</sub>(B<sup>3</sup>Π<sub>g</sub>) and N<sub>2</sub><sup>+</sup>(A<sup>2</sup>Π<sub>u</sub>) vibrational distributions observed in sprites. *J. Atmos. Sol.-Terr. Phys.* **65**, 583–590 (2003)
- E.J. Bucsela, K.E. Pickering, T.L. Huntemann, R.C. Cohen, A. Perring, J.F. Gleason, R.J. Blakeslee, R.I. Albrecht, R. Holzworth, J.P. Cipriani, D. Vargas-Navarro, I. Mora-Segura, A. Pacheco-Hernandez, S. Laporte-Molina, Lightning-generated NO<sub>x</sub> seen by the Ozone Monitoring Instrument during NASA's Tropical Composition, Cloud and Climate Coupling Experiment (TC4). *J. Geophys. Res.* **115**, D00J10 (2010). doi:[10.1029/2009JD013118](https://doi.org/10.1029/2009JD013118)
- L. Campbell, D.C. Cartwright, M.J. Brunger, Role of excited N<sub>2</sub> in the production of nitric oxide. *J. Geophys. Res.* **112**, A08303 (2007). doi:[10.1029/2007JA012337](https://doi.org/10.1029/2007JA012337)
- M. Carlotti, G. Brizzi, G. Papandrea, M. Prevedelli, M. Ridolfi, B. Dinelli, L. Magnani, GMTR: Two-dimensional geo-fit multitarget retrieval model for Michelson interferometer for passive atmospheric sounding/environmental satellite observations. *Appl. Opt.* **45**(4), 716–727 (2006)
- S. Celestin, V.P. Pasko, Effects of spatial non-uniformity of streamer discharges on spectroscopic diagnostics of peak electric fields in transient luminous events. *Geophys. Res. Lett.* **37**, L07804 (2010)
- S. Celestin, V.P. Pasko, Energy and fluxes of thermal runaway electrons produced by exponential growth of streamers during the stepping of lightning leaders and in transient luminous events. *J. Geophys. Res.* **116**, A03315 (2011)
- M. Černák, E.M. van Veldhuizen, I. Morva, W.R. Rutgers, Effect of cathode surface properties on glow-to-arc transition in a short positive corona gap in ambient air. *J. Phys. D, Appl. Phys.* **28**(6), 1126–1132 (1995)
- S.C. Chang, C.L. Kuo, L.J. Lee, A.B. Chen, H.T. Su, R.R. Hsu, H.U. Frey, S.B. Mende, Y. Takahashi, L.C. Lee, ISUAL far-ultraviolet events, elves, and lightning current. *J. Geophys. Res.* **115**, A00E46 (2010). doi:[10.1029/2009JA014861](https://doi.org/10.1029/2009JA014861)
- O. Chanrion, T. Neubert, A PIC-MCC code for simulation of streamer propagation in air. *J. Comput. Phys.* **227**(15), 7222–7245 (2008)
- O. Chanrion, T. Neubert, Production of runaway electrons by negative streamer discharges. *J. Geophys. Res.* **115**, A00E32 (2010). doi:[10.1029/2009JA014774](https://doi.org/10.1029/2009JA014774)
- A.B. Chen, C.L. Kuo, Y.J. Lee, H.T. Su, R.R. Hsu, J.L. Chern, H.U. Frey, S.B. Mende, Y. Takahashi, H. Fuku-nishi, Y.S. Chang, T.Y. Liu, L.C. Lee, Global distributions and occurrence rates of transient luminous events. *J. Geophys. Res.* **113**(A8), A08306 (2008)
- Z. Cheng, S.A. Cummer, H.T. Su, R.R. Hsu, Broadband very low frequency measurement of D region iono-spheric perturbations caused by lightning electromagnetic pulses. *J. Geophys. Res.* **112**(A6), A06318 (2007)

- J.L. Chern, R.R. Hsu, H.T. Su, S.B. Mende, H. Fukunishi, Y. Takahashi, L.C. Lee, Global survey of upper atmospheric transient luminous events on the ROCSAT-2 satellite. *J. Atmos. Sol.-Terr. Phys.* **65**, 647–659 (2003). doi:[10.1016/S1364-6826\(02\)00317-6](https://doi.org/10.1016/S1364-6826(02)00317-6)
- J.K. Chou, C.L. Kuo, L.Y. Tsai, A.B. Chen, H.T. Su, R.R. Hsu, S.A. Cummer, J. Li, H.U. Frey, S.B. Mende, Y. Takahashi, L.C. Lee, Gigantic jets with negative and positive polarity streamers. *J. Geophys. Res.* **115**, A00E45 (2010). doi:[10.1029/2009JA014831](https://doi.org/10.1029/2009JA014831)
- H. Christian, R. Blakeslee, D. Boccippio, W. Boeck, D. Buechler, K. Driscoll, S. Goodman, J. Hall, W. Koshak, D. Mach, M. Stewart, Global frequency and distribution of lightning as observed from space by the Optical Transient Detector. *J. Geophys. Res.* **108**(D1), 4005 (2003). doi:[10.1029/2002JD002347](https://doi.org/10.1029/2002JD002347)
- V. Cooray, M. Rahman, V. Rakov, On the  $\text{NO}_x$  production by laboratory electrical discharges and lightning. *J. Atmos. Sol.-Terr. Phys.* **71**(17–18), 1877–1889 (2009). doi:[10.1016/j.jastp.2009.07.009](https://doi.org/10.1016/j.jastp.2009.07.009)
- S.A. Cummer, Current moment in sprite-producing lightning. *J. Atmos. Sol.-Terr. Phys.* **65**, 499–508 (2003)
- S.A. Cummer, M. Fullekrug, Unusually intense continuing current in lightning produces delayed mesospheric breakdown. *Geophys. Res. Lett.* **28**, 495–498 (2001)
- S.A. Cummer, W.A. Lyons, Lightning charge moment changes in U.S. high plains thunderstorms. *Geophys. Res. Lett.* **31**(5), L05114 (2004). doi:[10.1029/2003GL019043](https://doi.org/10.1029/2003GL019043)
- S.A. Cummer, W.A. Lyons, Implication of lightning charge moment changes for sprite initiation. *J. Geophys. Res.* **110**, A04304 (2005). doi:[10.1029/2004JA010812](https://doi.org/10.1029/2004JA010812)
- S.A. Cummer, U.S. Inan, T.F. Bell, C.P. Barrington-Leigh, ELF radiation produced by electrical currents in sprites. *Geophys. Res. Lett.* **25**, 1281–1284 (1998)
- S.A. Cummer, H.U. Frey, S.B. Mende, R.R. Hsu, H.T. Su, A.B. Chen, H. Fukunishi, Y. Takahashi, Simultaneous radio and satellite optical measurements of high-altitude sprite current and lightning continuing current. *J. Geophys. Res.* **111**(A10), A10315 (2006a)
- S.A. Cummer, N.C. Jaugey, J.B. Li, W.A. Lyons, T.E. Nelson, E.A. Gerken, Submillisecond imaging of sprite development and structure. *Geophys. Res. Lett.* **33**, L04104 (2006b). doi:[10.1029/2005GL024969](https://doi.org/10.1029/2005GL024969)
- S.A. Cummer, J. Li, F. Han, G. Lu, N. Jaugey, W.A. Lyons, T.E. Nelson, Quantification of the troposphere-to-ionosphere charge transfer in a gigantic jet. *Nat. Geosci.* **2**, 1–4 (2009). doi:[10.1038/NGEO607](https://doi.org/10.1038/NGEO607)
- C. de Groot-Hedlin, Finite-difference time-domain synthesis of infrasound propagation through an absorbing atmosphere. *J. Acoust. Soc. Am.* **124**(3, Part 1), 1430–1441 (2008). doi:[10.1121/1.2959736](https://doi.org/10.1121/1.2959736)
- S. de Larquier, V.P. Pasko, Mechanism of inverted-chirp infrasonic radiation from sprites. *Geophys. Res. Lett.* **37**, L24803 (2010)
- J. de Urquijo, F.J. Gordillo-Vazquez, Comment on “ $\text{NO}_x$  production in laboratory discharges simulating blue jets and red sprites” by Harold Peterson et al. *J. Geophys. Res.* **115**, A12319 (2010). doi:[10.1029/2010JA015966](https://doi.org/10.1029/2010JA015966)
- S.K. Dhali, P.F. Williams, Two-dimensional studies of streamers in gases. *J. Appl. Phys.* **62**, 4696–4707 (1987)
- U. Ebert, D. Sentman, Editorial Review: Streamers, sprites, leaders, lightning: from micro- to macroscales. *J. Phys. D, Appl. Phys.* **41**, 230301 (2008)
- U. Ebert, C. Montijn, T.M.P. Briels, W. Hundsdorfer, B. Meulenbroek, A. Rocco, E.M. van Veldhuizen, The multiscale nature of streamers. *Plasma Sources Sci. Technol.* **15**, S118–S129 (2006)
- U. Ebert, S. Nijdam, C. Li, A. Luque, T. Briels, E. van Veldhuizen, Review of recent results on streamer discharges and discussion of their relevance for sprites and lightning. *J. Geophys. Res.* **115**, A00E43 (2010)
- C.F. Enell, A. Arnone, T. Adachi, O. Chanrion, P.T. Verronen, A. Seppala, T. Neubert, T. Ulich, E. Turunen, Y. Takahashi, R.R. Hsu, Parameterisation of the chemical effect of sprites in the middle atmosphere. *Ann. Geophys.* **26**, 13–27 (2008)
- T. Farges, E. Blanc, Characteristics of infrasound from lightning and sprites near thunderstorm areas. *J. Geophys. Res.* **115**, A00E31 (2010). doi:[10.1029/2009JA014700](https://doi.org/10.1029/2009JA014700)
- T. Farges, E. Blanc, A.L. Pichon, T. Neubert, T.H. Allin, Identification of infrasound produced by sprites during the Sprite2003 campaign. *Geophys. Res. Lett.* **32**(1), L01813 (2005). doi:[10.1029/2004GL021212](https://doi.org/10.1029/2004GL021212)
- H. Fischer, M. Birk, C. Blom, B. Carli, M. Carlotti, T. von Clarmann, L. Delbouille, A. Dudhia, D. Ehalt, M. Endemann, J.M. Flaud, R. Gessner, A. Kleinert, R. Koopman, J. Langen, M. Lopez-Puertas, P. Mosner, H. Nett, H. Oelhaf, G. Perron, J. Remedios, M. Ridolfi, G. Stiller, R. Zander, MIPAS: an instrument for atmospheric and climate research. *Atmos. Chem. Phys.* **8**(8), 2151–2188 (2008)
- G.J. Fishman, P.N. Bhat, R. Mallozzi, J.M. Horack, T. Koshut, C. Kouveliotou, G.N. Pendleton, C.A. Meegan, R.B. Wilson, W.S. Paciesas, S.J. Goodman, H.J. Christian, Discovery of intense gamma-ray flashes of atmospheric origin. *Science* **264**(5163), 1313–1316 (1994)
- R.C. Franz, R.J. Nemzek, J.R. Winckler, Television image of a large upward electric discharge above a thunderstorm system. *Science* **249**, 48–51 (1990)
- H.U. Frey, S.B. Mende, S.A. Cummer, A.B. Chen, R.R. Hsu, H.T. Su, Y.S. Chang, T. Adachi, H. Fukunishi, Y. Takahashi, Beta-type stepped leader of elve-producing lightning. *Geophys. Res. Lett.* **32**, L13824 (2005). doi:[10.1029/2005GL023080](https://doi.org/10.1029/2005GL023080)

- H.U. Frey, S.B. Mende, S.A. Cummer, J. Li, T. Adachi, H. Fukunishi, Y. Takahashi, A.B. Chen, R.R. Hsu, H.T. Su, Y.S. Chang, Halos generated by negative cloud-to-ground lightning. *Geophys. Res. Lett.* **34**, L18801 (2007)
- H. Fukunishi, Y. Takahashi, M. Kubota, K. Sakanoi, U.S. Inan, W.A. Lyons, Elves: Lightning-induced transient luminous events in the lower ionosphere. *Geophys. Res. Lett.* **23**(16), 2157–2160 (1996)
- H. Fukunishi, Y. Hiraki, T. Adachi, L. Tong, K. Nanbu, Occurrence conditions for gigantic jets connecting the thundercloud and the ionosphere. *Eos Trans. AGU* **86**(52), AE11A-02 (2005). Fall Meet. Suppl., Abstract AE11A-02
- M. Fullekrug, M.J. Rycroft, The contribution of sprites to the global atmospheric electric circuit. *Earth Planets Space* **58**(9), 1193–1196 (2006)
- M. Fullekrug, E.A. Mareev, M.J. Rycroft, *Sprites, Elves and Intense Lightning Discharges*. NATO Science Series II: Mathematics, Physics and Chemistry, vol. 225 (Springer, Heidelberg, 2006)
- W.R. Gamerota, S.A. Cummer, J. Li, H.C. Stenbaek-Nielsen, R.K. Haaland, M.G. McHarg, Comparison of sprite initiation altitudes between observations and models. *J. Geophys. Res.* **116**, A02317 (2011). doi:[10.1029/2010JA016095](https://doi.org/10.1029/2010JA016095)
- G. Garipov, B. Khrenov, M. Panasyuk, V. Tulupov, A. Shirokov, I. Yashin, H. Salazar, UV radiation from the atmosphere: results of the MSU “Tatiana” satellite measurements. *Astropart. Phys.* **24**(4–5), 400–408 (2005a). doi:[10.1016/j.astropartphys.2005.09.001](https://doi.org/10.1016/j.astropartphys.2005.09.001)
- G. Garipov, M. Panasyuk, V. Tulupov, B. Khrenov, A. Shirokov, I. Yashin, H. Salazar, Ultraviolet flashes in the equatorial region of the earth. *JETP Lett.* **82**(4), 185–187 (2005b)
- G. Garipov, M. Panasyuk, I. Rubinshtein, V. Tulupov, B. Khrenov, A. Shirokov, I. Yashin, H. Salazar, Ultraviolet radiation detector of the MSU research educational microsatellite Universitetskii-Tat’yana. *Instrum. Exp. Tech.* **49**(1), 126–131 (2006). doi:[10.1134/S0020441206010180](https://doi.org/10.1134/S0020441206010180)
- G.K. Garipov, B.A. Khrenov, M.I. Panasyuk, Correlation of atmospheric UV transient events with lunar phase. *Geophys. Res. Lett.* **35**(10), L18087 (2008). doi:[10.1029/2007GL032679](https://doi.org/10.1029/2007GL032679)
- G.K. Garipov, B.A. Khrenov, P.A. Klimov, V.S. Morozenko, M.I. Panasyuk, S.N. Petrova, V.I. Tulupov, V.M. Shahparonov, S.I. Svertilov, N.N. Vedenkin, I.V. Yashin, J.A. Jeon, S.M. Jeong, A.R. Jung, J.E. Kim, J. Lee, H.Y. Lee, G.W. Na, J.W. Nam, S. Nam, I.H. Park, J.E. Suh, J.Y. Jin, M. Kim, Y.K. Kim, B.W. Yoo, Y.S. Park, H.J. Yu, C.H. Lee, J.H. Park, H.I. Salazar, O.B. Martinez, E.L. Ponce, J.P. Cotsomi, Program of transient UV event research at Tatiana-2 satellite. *J. Geophys. Res.* **115**, A00E24 (2010). doi:[10.1029/2009JA014765](https://doi.org/10.1029/2009JA014765)
- E.A. Gerken, U.S. Inan, Observations of decameter-scale morphologies in sprites. *J. Atmos. Sol.-Terr. Phys.* **65**, 567–572 (2003). doi:[10.1016/S1364-6826\(02\)00333-4](https://doi.org/10.1016/S1364-6826(02)00333-4)
- E.A. Gerken, U.S. Inan, C.P. Barrington-Leigh, Telescopic imaging of sprites. *Geophys. Res. Lett.* **27**, 2637–2640 (2000)
- F.J. Gordillo-Vazquez, Air plasma kinetics under the influence of sprites. *J. Phys. D, Appl. Phys.* **41**(23), 234016 (2008)
- F.J. Gordillo-Vazquez, Z. Donko, Electron energy distribution functions and transport coefficients relevant for air plasmas in the troposphere: impact of humidity and gas temperature. *Plasma Sources Sci. Technol.* **18**, 034021 (2009)
- F.J. Gordillo-Vazquez, A. Luque, Electrical conductivity in sprite streamer channels. *Geophys. Res. Lett.* **37**, L16809 (2010). doi:[10.1029/2010GL044349](https://doi.org/10.1029/2010GL044349)
- E. Greenberg, C. Price, Y. Yair, M. Ganot, J. Bor, G. Satori, ELF transients associated with sprites and elves in eastern Mediterranean winter thunderstorms. *J. Atmos. Sol.-Terr. Phys.* **69**(13), 1569–1586 (2007). doi:[10.1016/j.jastp.2007.06.002](https://doi.org/10.1016/j.jastp.2007.06.002)
- C. Haldoupis, A. Mika, S. Shalimov, Modeling the relaxation of early VLF perturbations associated with transient luminous events. *J. Geophys. Res.* **114**, A00E04 (2009)
- C. Haldoupis, N. Amvrosiadi, B.R.T. Cotts, O.A. van der Velde, O. Chanrion, T. Neubert, More evidence for a one-to-one correlation between sprites and early VLF perturbations. *J. Geophys. Res.* **115**, A07304 (2010)
- M.J. Heavner, D.D. Sentman, D.R. Moudry, E.M. Wescott, Sprites, blue jets, and elves: optical evidence of energy transport across the stratopause, in *Atmospheric Science Across the Stratopause*, ed. by D.E. Siskind, S.D. Eckermann, M.E. Summers. Geophysical Monograph Series, vol. 123 (American Geophysical Union, Washington, 2000), pp. 69–82
- Y. Hiraki, Effects of ion-neutral chemical reactions on dynamics of lightning-induced electric field. *Plasma Sources Sci. Technol.* **18**(3), 034020 (2009)
- Y. Hiraki, H. Fukunishi, Theoretical criterion of charge moment change by lightning for initiation of sprites. *J. Geophys. Res.* **111**(A11), A11305 (2006)
- Y. Hiraki, Y. Kasai, H. Fukunishi, Chemistry of sprite discharges through ion-neutral reactions. *Atmos. Chem. Phys.* **8**(14), 3919–3928 (2008)

- R.R. Hsu, A.B. Chen, C. Kuo, Y. Lee, H.T. Su, H. Fukunishi, Y. Takahashi, T. Adachi, K. Yamamoto, H.U. Frey, S.B. Mende, L.C. Lee, Gigantic jet observation by the ISUAL payload of FORMOSAT-2 satellite. *Eos Trans. AGU* **86**(52), AE23A-0992 (2005). Fall Meet. Suppl., Abstract AE23A-0992
- R.R. Hsu, A.B. Chen, C.-L. Kuo, H.-T. Su, H. Frey, S. Mende, Y. Takahashi, L.-C. Lee, On the global occurrence and impacts of transient luminous events (TLEs). *AIP Conf. Proc.* **1118**(1), 99–107 (2009)
- W.Y. Hu, S.A. Cummer, W.A. Lyons, Lightning charge moment changes for the initiation of sprites. *Geophys. Res. Lett.* **29**(8), 1279 (2002). doi:[10.1029/2001GL014593](https://doi.org/10.1029/2001GL014593)
- W.Y. Hu, S.A. Cummer, W.A. Lyons, Testing sprite initiation theory using lightning measurements and modeled electromagnetic fields. *J. Geophys. Res.* **112**(D13), D13115 (2007)
- T.Y. Huang, C.Y. Chiang, C.L. Kuo, A.B. Chen, H.T. Su, R.R. Hsu, Investigations of lightning-induced sudden brightening in the OH airglow layer observed by ISUAL onboard FORMOSAT-II satellite. *AIP Conf. Proc.* **1118**(1), 21–27 (2009)
- T.-Y. Huang, C.L. Kuo, C.Y. Chiang, A.B. Chen, H.T. Su, R.R. Hsu, Further investigations of lightning-induced transient emissions in the OH airglow layer. *J. Geophys. Res.* **115**, A10326 (2010). doi:[10.1029/2010JA015558](https://doi.org/10.1029/2010JA015558)
- M. Ignaccolo, T. Farges, A. Mika, T.H. Allin, O. Chanrion, E. Blanc, T. Neubert, A.C. Fraser-Smith, M. Fullekrug, The planetary rate of sprite events. *Geophys. Res. Lett.* **33**(11), L11808 (2006)
- U.S. Inan, Lightning effects at high altitudes: sprites, elves, and terrestrial gamma ray flashes. *C. R. Phys.* **3**(10), 1411–1421 (2002)
- U.S. Inan, T.F. Bell, J.V. Rodriguez, Heating and ionization of the lower ionosphere by lightning. *Geophys. Res. Lett.* **18**(4), 705–708 (1991)
- U.S. Inan, C. Barrington-Leigh, S. Hansen, V.S. Glukhov, T.F. Bell, R. Rairden, Rapid lateral expansion of optical luminosity in lightning-induced ionospheric flashes referred to as ‘elves’. *Geophys. Res. Lett.* **24**(5), 583–586 (1997)
- U.S. Inan, S.A. Cummer, R.A. Marshall, A survey of elf and VLF research on lightning-ionosphere interactions and causative discharges. *J. Geophys. Res.* **115**, A00E36 (2010)
- P. Israelevich, Y. Yair, A. Devir, J. Joseph, Z. Levin, I. Mayo, M. Moalem, C. Price, B. Ziv, A. Sternlieb, Transient airglow enhancements observed from the space shuttle Columbia during the MEIDEX sprite campaign. *Geophys. Res. Lett.* **31**(6), L06124 (2004). doi:[10.1029/2003GL019110](https://doi.org/10.1029/2003GL019110)
- T. Kanmae, H.C. Stenbaek-Nielsen, M.G. McHarg, Altitude resolved sprite spectra with 3 ms temporal resolution. *Geophys. Res. Lett.* **34**, L07810 (2007)
- H.W. Kasemir, A contribution to the electrostatic theory of a lightning discharge. *J. Geophys. Res.* **65**(7), 1873–1878 (1960)
- S.I. Klimov, E.A. Sharkov, L.M. Zelenyi, The tropical cyclones as the possible sources of gamma emission in the Earth’s atmosphere. *Eos Trans. AGU* **90**, 52 (2009). Abstract AE33B-0295
- P.R. Krehbiel, J.A. Rioussel, V.P. Pasko, R.J. Thomas, W. Rison, M.A. Stanley, H.E. Edens, Upward electrical discharges from thunderstorms. *Nat. Geosci.* **1**(4), 233–237 (2008). doi:[10.1038/ngel162](https://doi.org/10.1038/ngel162)
- C.L. Kuo, R.R. Hsu, H.T. Su, A.B. Chen, L.C. Lee, S.B. Mende, H.U. Frey, H. Fukunishi, Y. Takahashi, Electric fields and electron energies inferred from the ISUAL recorded sprites. *Geophys. Res. Lett.* **32**, L19103 (2005). doi:[10.1029/2005GL023389](https://doi.org/10.1029/2005GL023389)
- C.L. Kuo, A.B. Chen, R.R. Hsu, H.T. Su, L.C. Lee, S.B. Mende, H.U. Frey, H. Fukunishi, Y. Takahashi, Analysis of ISUAL recorded gigantic jets, in *Abstracts of Workshop on Streamers, Sprites, Leaders, Lightning: From Micro- to Macroscales*, Lorentz Center, Leiden University, 8–12 October 2007 (2007a)
- C.L. Kuo, A.B. Chen, Y.J. Lee, L.Y. Tsai, R.K. Chou, R.R. Hsu, H.T. Su, L.C. Lee, S.A. Cummer, H.U. Frey, S.B. Mende, Y. Takahashi, H. Fukunishi, Modeling elves observed by FORMOSAT-2 satellite. *J. Geophys. Res.* **112**, A11312 (2007b)
- C.L. Kuo, A.B. Chen, J.K. Chou, L.Y. Tsai, R.R. Hsu, H.T. Su, H.U. Frey, S.B. Mende, Y. Takahashi, L.C. Lee, Radiative emission and energy deposition in transient luminous events. *J. Phys. D, Appl. Phys.* **41**, 234014 (2008)
- C.L. Kuo, J.K. Chou, L.Y. Tsai, A.B. Chen, H.T. Su, R.R. Hsu, S.A. Cummer, H.U. Frey, S.B. Mende, Y. Takahashi, L.C. Lee, Discharge processes, electric field, and electron energy in ISUAL-recorded gigantic jets. *J. Geophys. Res.* **114**, A04314 (2009)
- A. Larsson, The effect of a large series resistance on the streamer-to-spark transition in dry air. *J. Phys. D, Appl. Phys.* **31**(9), 1100 (1998)
- E.H. Lay, C.J. Rodger, R.H. Holzworth, M. Cho, J.N. Thomas, Temporal-spatial modeling of electron density enhancement due to successive lightning strokes. *J. Geophys. Res.* **115**(0), A00E59 (2010)
- F. Leblanc, K.L. Aplin, Y. Yair, R.G. Harrison, J.P. Lebreton, M. Blanc, *Planetary atmospheric electricity* 532 pp. (Springer, Berlin, 2008)
- L.-J. Lee, A.B. Chen, S.-C. Chang, C.-L. Kuo, H.-T. Su, R.-R. Hsu, C.-C. Wu, P.-H. Lin, H.U. Frey, S.B. Mende, Y. Takahashi, L.-C. Lee, Controlling synoptic-scale factors for the distribution of transient luminous events. *J. Geophys. Res.* **115**, A00E54 (2010). doi:[10.1029/2009JA014823](https://doi.org/10.1029/2009JA014823)

- F. Lefevvre, E. Blanc, J.L.P.T. Team, TARANIS—a satellite project dedicated to the physics of TLEs and TGFs. AIP Conf. Proc. **1118**(1), 3–7 (2009)
- C. Li, U. Ebert, W. Hundsdoerfer, 3D hybrid computations for streamer discharges and production of runaway electrons. J. Phys. D, Appl. Phys. **42**(20), 202003 (2009). doi:[10.1088/0022-3727/42/20/202003](https://doi.org/10.1088/0022-3727/42/20/202003)
- J. Li, S. Cummer, Estimation of electric charge in sprites from optical and radio observations. J. Geophys. Res. **116**, A01301 (2011). doi:[10.1029/2010JA015391](https://doi.org/10.1029/2010JA015391)
- J. Li, S.A. Cummer, W.A. Lyons, T.E. Nelson, Coordinated analysis of delayed sprites with high-speed images and remote electromagnetic fields. J. Geophys. Res. **113**(D20), D20206 (2008)
- C. Liu, E.R. Williams, E.J. Zipser, G. Burns, Diurnal variations of global thunderstorms and electrified shower clouds and their contribution to the global electrical circuit. J. Atmos. Sci. **67**(2), 309–323 (2010). doi:[10.1175/2009JAS3248.1](https://doi.org/10.1175/2009JAS3248.1)
- N. Liu, Model of sprite luminous trail caused by increasing streamer current. Geophys. Res. Lett. **37**, L04102 (2010). doi:[10.1029/2009GL042214](https://doi.org/10.1029/2009GL042214)
- N.Y. Liu, V.P. Pasko, Effects of photoionization on propagation and branching of positive and negative streamers in sprites. J. Geophys. Res. **109**, A04301 (2004). doi:[10.1029/2003JA010064](https://doi.org/10.1029/2003JA010064)
- N.Y. Liu, V.P. Pasko, Molecular nitrogen LBH band system far-UV emissions of sprite streamers. Geophys. Res. Lett. **32**, L05104 (2005). doi:[10.1029/2004GL022001](https://doi.org/10.1029/2004GL022001)
- N.Y. Liu, V.P. Pasko, Modeling studies of NO- $\gamma$  emissions of sprites. Geophys. Res. Lett. **34**, L16103 (2007)
- N.Y. Liu, V.P. Pasko, No-gamma emissions from streamer discharges: direct electron impact excitation versus resonant energy transfer. J. Phys. D, Appl. Phys. **43**, 082001 (2010)
- N.Y. Liu, V.P. Pasko, D.H. Burkhardt, H.U. Frey, S.B. Mende, H.-T. Su, A.B. Chen, R.-R. Hsu, L.-C. Lee, H. Fukunishi, Y. Takahashi, Comparison of results from sprite streamer modeling with spectrophotometric measurements by ISUAL instrument on FORMOSAT-2 satellite. Geophys. Res. Lett. **33**, L01101 (2006). doi:[10.1029/2005GL024243](https://doi.org/10.1029/2005GL024243)
- N.Y. Liu, V.P. Pasko, K. Adams, H.C. Stenbaek-Nielsen, M.G. McHarg, Comparison of acceleration, expansion, and brightness of sprite streamers obtained from modeling and high-speed video observations. J. Geophys. Res. **114**, A00E03 (2009a)
- N.Y. Liu, V.P. Pasko, H.U. Frey, S.B. Mende, H.-T. Su, A.B. Chen, R.-R. Hsu, L.-C. Lee, Assessment of sprite initiating electric fields and quenching altitude of a  $^1\pi_g$  state of  $n_2$  using sprite streamer modeling and ISUAL spectrophotometric measurements. J. Geophys. Res. **114**, A00E02 (2009b)
- G. Lu, S.A. Cummer, J. Li, F. Han, R.J. Blakeslee, H.J. Christian, Charge transfer and in-cloud structure of large-charge-moment positive lightning strokes in a mesoscale convective system. Geophys. Res. Lett. **36**, L15805 (2009). doi:[10.1029/2009GL038880](https://doi.org/10.1029/2009GL038880)
- G. Lu, R.J. Blakeslee, J. Li, D.M. Smith, X.M. Shao, E.W. McCaul, D.E. Buechler, H.J. Christian, J.M. Hall, S.A. Cummer, Lightning mapping observation of a terrestrial gamma-ray flash. Geophys. Res. Lett. **37**, L11806 (2010). doi:[10.1029/2010GL043494](https://doi.org/10.1029/2010GL043494)
- G. Lu, S.A. Cummer, J. Li, F. Han, D.M. Smith, B.W. Grefenstette, Characteristics of broadband lightning emissions associated with terrestrial gamma ray flashes. J. Geophys. Res. **116**, A03316 (2011a). doi:[10.1029/2010JA016141](https://doi.org/10.1029/2010JA016141)
- G. Lu, S.A. Cummer, W.A. Lyons, P.R. Krehbiel, J. Li, W. Rison, R.J. Thomas, H.E. Edens, M.A. Stanley, W. Beasley, D.R. MacGorman, O.A. van der Velde, M.B. Cohen, T.J. Lang, S.A. Rutledge, Lightning development associated with two negative gigantic jets. Geophys. Res. Lett. **38**, L12801 (2011b). doi:[10.1029/2011GL047662](https://doi.org/10.1029/2011GL047662)
- A. Luque, U. Ebert, Emergence of sprite streamers from screening-ionization waves in the lower ionosphere. Nat. Geosci. **2**(11), 757–760 (2009). doi:[10.1038/NGEO662](https://doi.org/10.1038/NGEO662)
- A. Luque, U. Ebert, Sprites in varying air density: charge conservation, glowing negative trails and changing velocity. Geophys. Res. Lett. **37**, L06806 (2010). doi:[10.1029/2009GL041982](https://doi.org/10.1029/2009GL041982)
- A. Luque, F.J. Gordillo-Vazquez, Sprite beads originating from inhomogeneities in the mesospheric electron density. Geophys. Res. Lett. **38**, L04808 (2011). doi:[10.1029/2010GL046403](https://doi.org/10.1029/2010GL046403)
- W.A. Lyons, Sprite observations above the U.S. high plains in relation to their parent thunderstorm systems. J. Geophys. Res. **101**, 29641–29652 (1996)
- W.A. Lyons, The meteorology of transient luminous events—an introduction and overview, in *Sprites, Elves and Intense Lightning Discharges*, ed. by M. Füllekrug, E.A. Mareev, M.J. Rycroft. NATO Science Series II: Mathematics, Physics and Chemistry, vol. 225 (Springer, Heidelberg, 2006), pp. 19–56
- W.A. Lyons, T.E. Nelson, R.A. Armstrong, V.P. Pasko, M.A. Stanley, Upward electrical discharges from thunderstorm tops. Bull. Am. Meteorol. Soc. **84**(4), 445–454 (2003). doi:[10.1175/BAMS-84-4-445](https://doi.org/10.1175/BAMS-84-4-445)
- W.A. Lyons, M.A. Stanley, J.D. Meyer, T.E. Nelson, S.A. Rutledge, T. Lang, S.A. Cummer, The meteorological and electrical structure of TLE-producing convective storms, in *Lightning: Principles, Instruments and Applications*, ed. by H. Betz, U. Schumann, P. Laroche (Springer, Berlin, 2009), pp. 387–415
- W.A. Lyons, M.A. Stanley, T.E. Nelson, S.A. Cummer, C.R. Huffines, K.C. Wiens, Supercells and sprites. Bull. Am. Meteorol. Soc. **89**(8), 1165+ (2008). doi:[10.1175/2008BAMS2439.1](https://doi.org/10.1175/2008BAMS2439.1)



- E.A. Mareev, Global electric circuit research: achievements and prospects. *Phys. Usp.* **53**(5), 504–511 (2010). doi:[10.3367/UFNe.0180.201005h.0527](https://doi.org/10.3367/UFNe.0180.201005h.0527)
- E.A. Mareev, S.A. Yashunin, S.S. Davydenko, T.C. Marshall, M. Stolzenburg, C.R. Maggio, On the role of transient currents in the global electric circuit. *Geophys. Res. Lett.* **35**(15), L15810 (2008). doi:[10.1029/2008GL034554](https://doi.org/10.1029/2008GL034554)
- R.A. Marshall, U.S. Inan, High-speed measurements of small-scale features in sprites: Sizes and lifetimes. *Radio Sci.* **41**, RS6S43 (2006). doi:[10.1029/2005RS003353](https://doi.org/10.1029/2005RS003353)
- R.A. Marshall, U.S. Inan, Two-dimensional frequency domain modeling of lightning EMP-induced perturbations to VLF transmitter signals. *J. Geophys. Res.* **115**, A00E29 (2010)
- R.A. Marshall, U.S. Inan, V.S. Glukhov, Elves and associated electron density changes due to cloud-to-ground and in-cloud lightning discharges. *J. Geophys. Res.* **115**, A00E17 (2010)
- J.D. Mathews, M.A. Stanley, V.P. Pasko, T.G. Wood, U.S. Inan, M.J. Heavner, S.A. Cummer, Electromagnetic signatures of the Puerto Rico blue jet and its parent thunderstorm. *Eos Trans. AGU* **83**(47) (2002). Fall Meet. Suppl., Abstract A62D-02
- Y. Matsudo, I. Suzuki, K. Michimoto, K. Myokei, M. Hayakawa, Comparison of time delays of sprites induced by winter lightning flashes in the Japan Sea with those in the Pacific Ocean. *J. Atmos. Sol.-Terr. Phys.* **71**(1), 101–111 (2009). doi:[10.1016/j.jastp.2008.09.040](https://doi.org/10.1016/j.jastp.2008.09.040)
- V. Mazur, L.H. Ruhnke, Model of electric charges in thunderstorms and associated lightning. *J. Geophys. Res.* **103**(D18), 23299–23308 (1998)
- M.G. McHarg, H.C. Stenbaek-Nielsen, T. Kanmae, Streamer development in sprites. *Geophys. Res. Lett.* **34**, L06804 (2007). doi:[10.1029/2006GL027854](https://doi.org/10.1029/2006GL027854)
- S.B. Mende, H.U. Frey, R.R. Hsu, H.T. Su, A.B. Chen, L.C. Lee, D.D. Sentman, Y. Takahashi, H. Fukunishi, D region ionization by lightning-induced EMP. *J. Geophys. Res.* **110**, A11312 (2005). doi:[10.1029/2005JA011064](https://doi.org/10.1029/2005JA011064)
- S.B. Mende, Y.S. Chang, A.B. Chen, H.U. Frey, H. Fukunishi, S.P. Geller, S. Harris, H. Heeterdks, R.R. Hsu, L.C. Lee, H.T. Su, Y. Takahashi, Spacecraft based studies of transient luminous events, in *Sprites, Elves and Intense Lightning Discharges*, ed. by M. Füllekrug, E.A. Mareev, M.J. Rycroft. NATO Science Series II: Mathematics, Physics and Chemistry, vol. 225 (Springer, Heidelberg, 2006), pp. 123–149
- A. Mika, C. Haldoupis, T. Neubert, H.T. Su, R.R. Hsu, R.J. Steiner, R.A. Marshall, Early VLF perturbations observed in association with elves. *Ann. Geophys.* **24**(8), 2179–2189 (2006)
- G.M. Milikh, M.N. Shneider, Model of UV flashes due to gigantic blue jets. *J. Phys. D, Appl. Phys.* **41**(23), 234013 (2008)
- E.V. Mishin, G.M. Milikh, Blue jets: Upward lightning. *Space Sci. Rev.* **137**(1–4), 473–488 (2008)
- J. Montanya, O. van der Velde, D. Romero, V. March, G. Sola, N. Pineda, M. Arrayas, J.L. Trueba, V. Reglero, S. Soula, High-speed intensified video recordings of sprites and elves over the western Mediterranean Sea during winter thunderstorms. *J. Geophys. Res.* **115**, A00E18 (2010). doi:[10.1029/2009JA014508](https://doi.org/10.1029/2009JA014508)
- J.S. Merrill, E.J. Bucsela, V.P. Pasko, S.L. Berg, W.M. Benesch, E.M. Wescott, M.J. Heavner, Time resolved N<sub>2</sub> triplet state vibrational populations and emissions associated with red sprites. *J. Atmos. Sol.-Terr. Phys.* **60**, 811–829 (1998)
- G.D. Moss, V.P. Pasko, N.Y. Liu, G. Veronis, Monte Carlo model for analysis of thermal runaway electrons in streamer tips in transient luminous events and streamer zones of lightning leaders. *J. Geophys. Res.* **111**, A02307 (2006). doi:[10.1029/2005JA011350](https://doi.org/10.1029/2005JA011350)
- G.V. Naidis, Positive and negative streamers in air: velocity-diameter relation. *Phys. Rev. E* **79**(5, Part 2), 057401 (2009). doi:[10.1103/PhysRevE.79.057401](https://doi.org/10.1103/PhysRevE.79.057401)
- T. Neubert, On sprites and their exotic kin. *Science* **300**, 747–749 (2003)
- T. Neubert, ASIM—an Instrument Suite for the International Space Station. *AIP Conf. Proc.* **1118**(1), 8–12 (2009)
- T. Neubert, M. Rycroft, T. Farges, E. Blanc, O. Chanrion, E. Arnone, A. Odzimek, N. Arnold, C.F.E. CF, E. Turunen, T. Bosing, A. Mika, C. Haldoupis, R.J. Steiner, O. van der Velde, O. Soula, P. Berg, F. Boberg, P. Thejll, B. Christiansen, M. Ignaccolo, M. Füllekrug, P.T. Verronen, J. Montanya, N. Crosby, Recent results from studies of electric discharges in the mesosphere. *Surv. Geophys.* **29**(2), 71–137 (2008)
- S. Nijdam, J.S. Moerman, T.M.P. Briels, E.M. van Veldhuizen, U. Ebert, Stereo-photography of streamers in air. *Appl. Phys. Lett.* **92**(10), 101502 (2008). doi:[10.1063/1.2894195](https://doi.org/10.1063/1.2894195)
- S. Nijdam, E.M. van Veldhuizen, U. Ebert, Comment on “NO<sub>x</sub> production in laboratory discharges simulating blue jets and red sprites” by H. Peterson et al. *J. Geophys. Res.* **115**, A12305 (2010). doi:[10.1029/2010JA015861](https://doi.org/10.1029/2010JA015861)
- M.I. Panasyuk, V.V. Bogomolov, G.K. Garipov, O.R. Grigoryan, Y.I. Denisov, B.A. Khrenov, P.A. Klimov, L.L. Lazutin, S.I. Svertilov, N.N. Vedenkin, I.V. Yashin, S.I. Klimov, V.S. Makhmutov, Y.I. Stozkov, N.S. Svirzhevsky, V.V. Klimenko, E.A. Mareev, Y.V. Shlyugaev, V.E. Korepanov, I.H. Park, H.I. Salazar, H. Rothkaehl, Energetic particles impacting the upper atmosphere in connection with transient luminous event phenomena: Russian space experiment programs. *AIP Conf. Proc.* **1118**(1), 108–115 (2009)



- V. Pasko, U. Inan, T. Bell, Sprites as luminous columns of ionization produced by quasi-electrostatic thundercloud fields. *Geophys. Res. Lett.* **23**(6), 649–652 (1996)
- V.P. Pasko, Electric jets. *Nature* **423**, 927–929 (2003)
- V.P. Pasko, Theoretical modeling of sprites and jets, in *Sprites, Elves and Intense Lightning Discharges*, ed. by M. Füllekrug, E.A. Mareev, M.J. Rycroft. NATO Science Series II: Mathematics, Physics and Chemistry, vol. 225 (Springer, Heidelberg, 2006), pp. 253–311
- V.P. Pasko, Red sprite discharges in the atmosphere at high altitude: the molecular physics and the similarity with laboratory discharges. *Plasma Sources Sci. Technol.* **16**, S13–S29 (2007). doi:[10.1088/0963-0252/16/1/S02](https://doi.org/10.1088/0963-0252/16/1/S02)
- V.P. Pasko, Blue jets and gigantic jets: transient luminous events between thunderstorm tops and the lower ionosphere. *Plasma Phys. Control. Fusion* **50**, 124050 (2008)
- V.P. Pasko, Recent advances in theory of transient luminous events. *J. Geophys. Res.* **50**, A00E35 (2010)
- V.P. Pasko, A. Bourdon, Air heating associated with transient luminous events, in *Proc. 28th Int. Conf. On Phenomena in Ionized Gases (ICPIG), 5P07-12*, Institute of Plasma Physics, Prague, Czech Republic, 15–20 July 2007 (2007), pp. 1908–1911
- V.P. Pasko, J.J. George, Three-dimensional modeling of blue jets and blue starters. *J. Geophys. Res.* **107**(A12), 1458 (2002). doi:[10.1029/2002JA009473](https://doi.org/10.1029/2002JA009473)
- V.P. Pasko, H.C. Stenbaek-Nielsen, Diffuse and streamer regions of sprites. *Geophys. Res. Lett.* **29**(10), 1440 (2002). doi:[10.1029/2001GL014241](https://doi.org/10.1029/2001GL014241)
- V.P. Pasko, U.S. Inan, T.F. Bell, Heating, ionization and upward discharges in the mesosphere due to intense quasi-electrostatic thundercloud fields. *Geophys. Res. Lett.* **22**(4), 365–368 (1995)
- V.P. Pasko, U.S. Inan, T.F. Bell, Y.N. Taranenko, Sprites produced by quasi-electrostatic heating and ionization in the lower ionosphere. *J. Geophys. Res.* **102**(A3), 4529–4561 (1997). doi:[10.1029/96JA03528](https://doi.org/10.1029/96JA03528)
- V.P. Pasko, U.S. Inan, T.F. Bell, Spatial structure of sprites. *Geophys. Res. Lett.* **25**, 2123–2126 (1998a)
- V.P. Pasko, U.S. Inan, T.F. Bell, S.C. Reising, Mechanism of ELF radiation from sprites. *Geophys. Res. Lett.* **25**(18), 3493–3496 (1998b)
- V.P. Pasko, U. Inan, T. Bell, Large scale modeling of sprites and blue jets. *Eos Trans. AGU* **80**(46), F218 (1999). Fall Meet. Suppl., Abstract A42E-11
- V.P. Pasko, U.S. Inan, T.F. Bell, Fractal structure of sprites. *Geophys. Res. Lett.* **27**(4), 497–500 (2000). doi:[10.1029/1999GL010749](https://doi.org/10.1029/1999GL010749)
- V.P. Pasko, M.A. Stanley, J.D. Matthews, U.S. Inan, T.G. Wood, Electrical discharge from a thundercloud top to the lower ionosphere. *Nature* **416**, 152–154 (2002). doi:[10.1038/416152a](https://doi.org/10.1038/416152a)
- H. Peterson, M. Bailey, J. Hallett, W. Beasley,  $\text{NO}_x$  production in laboratory discharges simulating blue jets and red sprites. *J. Geophys. Res.* **114**, A00E07 (2009). doi:[10.1029/2009JA014489](https://doi.org/10.1029/2009JA014489)
- H. Peterson, M. Bailey, J. Hallett, W. Beasley, Reply to comment by S. Nijdam et al. on “ $\text{NO}_x$  production in laboratory discharges simulating blue jets and red sprites”. *J. Geophys. Res.* **115**, A12306 (2010a). doi:[10.1029/2010JA015946](https://doi.org/10.1029/2010JA015946)
- H. Peterson, M. Bailey, J. Hallett, W. Beasley, Reply to comment by J. de Urquijo and F. J. Gordillo-Vazquez on “ $\text{NO}_x$  production in laboratory discharges simulating blue jets and red sprites”. *J. Geophys. Res.* **115**, A12320 (2010b). doi:[10.1029/2010JA016040](https://doi.org/10.1029/2010JA016040)
- N.I. Petrov, G.N. Petrova, Physical mechanisms for the development of lightning discharges between a thundercloud and the ionosphere. *Tech. Phys.* **44**, 472–475 (1999)
- L. Pitchford, S. Oneil, J. Rumble, Extended Boltzmann analysis of electron swarm experiments. *Phys. Rev. A* **23**(1), 294–304 (1981)
- J. Qin, S. Celestin, V.P. Pasko, On the inception of streamers from sprite halo events produced by lightning discharges with positive and negative polarity. *J. Geophys. Res.* **116**, A06305 (2011)
- Y.P. Raizer, *Gas Discharge Physics* (Springer, New York, 1991)
- Y.P. Raizer, G.M. Milikh, M.N. Shneider, S.V. Novakovski, Long streamers in the upper atmosphere above thundercloud. *J. Phys. D, Appl. Phys.* **31**, 3255–3264 (1998)
- Y.P. Raizer, G.M. Milikh, M.N. Shneider, On the mechanism of blue jet formation and propagation. *Geophys. Res. Lett.* **33**(23), L23801 (2006). doi:[10.1029/2006GL027697](https://doi.org/10.1029/2006GL027697)
- Y.P. Raizer, G.M. Milikh, M.N. Shneider, Leader-streamers nature of blue jets. *J. Atmos. Sol.-Terr. Phys.* **69**(8), 925–938 (2007). doi:[10.1016/j.jastp.2007.02.007](https://doi.org/10.1016/j.jastp.2007.02.007)
- Y.P. Raizer, G.M. Milikh, M.N. Shneider, Streamer- and leader-like processes in the upper atmosphere: models of red sprites and blue jets. *J. Geophys. Res.* **115**, A00E42 (2010)
- V.A. Rakov, M.A. Uman, *Lightning: Physics and Effects* (Cambridge University Press, Cambridge, 2003)
- V.A. Rakov, D.E. Crawford, K.J. Rambo, G.H. Schnetzer, M.T.A. Uman, R. Thottappillil, M-component mode of charge transfer to ground in lightning discharge. *J. Geophys. Res.* **106**(D19), 22817–22831 (2001)
- J.A. Rioussel, V.P. Pasko, P.R. Krehbiel, R.J. Thomas, W. Rison, Three-dimensional fractal modeling of intracloud lightning discharge in a New Mexico thunderstorm and comparison with lightning mapping observations. *J. Geophys. Res.* **112**, D15203 (2007). doi:[10.1029/2006JD007621](https://doi.org/10.1029/2006JD007621)

- J.A. Riousset, V.P. Pasko, A. Bourdon, Air-density-dependent model for analysis of air heating associated with streamers, leaders, and transient luminous events. *J. Geophys. Res.* **115**, A12321 (2010a)
- J.A. Riousset, V.P. Pasko, P.R. Krehbiel, W. Rison, M.A. Stanley, Modeling of thundercloud screening charges: Implications for blue and gigantic jets. *J. Geophys. Res.* **115**, A00E10 (2010b)
- A. Rocco, U. Ebert, W. Hundsdoerfer, Branching of negative streamers in free flight. *Phys. Rev. E* **66**, 035102(R) (2002). doi:[10.1103/PhysRevE.66.035102](https://doi.org/10.1103/PhysRevE.66.035102)
- C.J. Rodger, Red sprites, upward lightning and VLF perturbations. *Rev. Geophys.* **37**, 317–336 (1999)
- C.J. Rodger, A. Seppala, M.A. Clilverd, Significance of transient luminous events to neutral chemistry: experimental measurements. *Geophys. Res. Lett.* **35**(7), L07803 (2008)
- R. Roussel-Dupre, J.J. Colman, E. Symbalisty, D. Sentman, V.P. Pasko, Physical processes related to discharges in planetary atmospheres. *Space Sci. Rev.* **137**(1–4), 51–82 (2008)
- H.L. Rowland, Theories and simulations of elves, sprites and blue jets. *J. Atmos. Sol.-Terr. Phys.* **60**, 831–844 (1998)
- M.J. Rycroft, A. Odzimek, Effects of lightning and sprites on the ionospheric potential, and threshold effects on sprite initiation, obtained using an analog model of the global atmospheric electric circuit. *J. Geophys. Res.* **115**, A00E37 (2010). doi:[10.1029/2009JA014758](https://doi.org/10.1029/2009JA014758)
- M. Sato, H. Fukunishi, Global sprite occurrence locations and rates derived from triangulation of transient Schumann resonance events. *Geophys. Res. Lett.* **30**(16), 1859 (2003). doi:[10.1029/2003GL017291](https://doi.org/10.1029/2003GL017291)
- M. Sato, T. Ushio, T. Morimoto, M. Suzuki, A. Yamazaki, K. Masayuki, R. Ishida, Y. Takahashi, U.S. Inan, Y. Hobara, Y. Sakamoto, K. Yoshida, H. Ishikawa, K. Yoshita, Science goal and mission status of JEM-GLIMS. *Eos Trans. AGU* **90**(52) (2009). Abstract AE23A-03
- U. Schumann, H. Huntrieser, The global lightning-induced nitrogen oxides source. *Atmos. Chem. Phys.* **7**(14), 3823–3907 (2007)
- D.D. Sentman, H.C. Stenbaek-Nielsen, Chemical effects of weak electric fields in the trailing columns of sprite streamers. *Plasma Sources Sci. Technol.* **18**(3), 034012 (2009)
- D.D. Sentman, E.M. Wescott, D.L. Osborne, D.L. Hampton, M.J. Heavner, Preliminary results from the Sprites94 campaign: Red sprites. *Geophys. Res. Lett.* **22**, 1205–1208 (1995)
- D.D. Sentman, E.M. Wescott, R.H. Picard, J.R. Winick, H.C. Stenbaek-Nielsen, E.M. Dewan, D.R. Moudry, F.T. São Sabbas, M.J. Heavner, J. Morrill, Simultaneous observations of mesospheric gravity waves and sprites generated by a Midwestern thunderstorm. *J. Atmos. Sol.-Terr. Phys.* **65**, 537–550 (2003)
- D.D. Sentman, H.C. Stenbaek-Nielsen, M.G. McHarg, J.S. Morrill, Plasma chemistry of sprite streamers. *J. Geophys. Res.* **113**, D11112 (2008)
- M.N. Shneider, G.M. Milikh, Analysis of UV flashes of millisecond scale detected by a low-orbit satellite. *J. Geophys. Res.* **115**, A00E23 (2010). doi:[10.1029/2009JA014685](https://doi.org/10.1029/2009JA014685)
- D. Siingh, A.K. Singh, R.P. Patel, R. Singh, R.P. Singh, B. Veenadhari, M. Mukherjee, Thunderstorms, lightning, sprites and magnetospheric whistler-mode radio waves. *Surv. Geophys.* **29**(6), 499–551 (2008)
- D.M. Smith, L.I. Lopez, R.P. Lin, C.P. Barrington-Leigh, Terrestrial gamma-ray flashes observed up to 20 MeV. *Science* **307**(5712), 1085–1088 (2005). doi:[10.1126/science.1107466](https://doi.org/10.1126/science.1107466)
- M. Stanley, P. Krehbiel, M. Brook, C. Moore, W. Rison, B. Abrahams, High speed video of initial sprite development. *Geophys. Res. Lett.* **26**, 3201–3204 (1999)
- M.A. Stanley, Sprites and their parent discharges. Ph.D. thesis, New Mexico Institute of Mining and Technology, Socorro, NM (2000)
- M.A. Stanley, W.A. Lyons, T.E. Nelson, P.R. Krehbiel, W. Rison, R.J. Thomas, Comparison of sprite locations with lightning channel structure. *Eos Trans. AGU* **88**(52) (2007). Fall Meet. Suppl., Abstract AE41A-07
- H.C. Stenbaek-Nielsen, M.G. McHarg, High time-resolution sprite imaging: observations and implications. *J. Phys. D, Appl. Phys.* **41**, 234009 (2008)
- H.C. Stenbaek-Nielsen, M.G. McHarg, T. Kanmae, D.D. Sentman, Observed emission rates in sprite streamer heads. *Geophys. Res. Lett.* **34**, L11105 (2007). doi:[10.1029/2007GL029881](https://doi.org/10.1029/2007GL029881)
- H.C. Stenbaek-Nielsen, R. Haaland, M.G. McHarg, B.A. Hensley, T. Kanmae, Sprite initiation altitude measured by triangulation. *J. Geophys. Res.* **115**, A00E12 (2010). doi:[10.1029/2009JA014543](https://doi.org/10.1029/2009JA014543)
- H.T. Su, R.R. Hsu, A.B. Chen, Y.C. Wang, W.S. Hsiao, W.C. Lai, L.C. Lee, M. Sato, H. Fukunishi, Gigantic jets between a thundercloud and the ionosphere. *Nature* **423**, 974–976 (2003). doi:[10.1038/nature01759](https://doi.org/10.1038/nature01759)
- A.I. Sukhorukov, P. Stubbe, Problems of blue jet theories. *J. Atmos. Sol.-Terr. Phys.* **23**(13), 7–9 (1998). doi:[10.1016/S1364-6826\(98\)00021-2](https://doi.org/10.1016/S1364-6826(98)00021-2)
- L. Sutherland, H. Bass, Atmospheric absorption in the atmosphere up to 160 km. *J. Acoust. Soc. Am.* **115**(3), 1012–1032 (2004). doi:[10.1121/1.1631937](https://doi.org/10.1121/1.1631937)
- Y. Takahashi, K. Yoshida, Y. Sakamoto, T. Sakamoi, SPRITE-SAT: A University Small Satellite for Observation of High-Altitude Luminous Events, in *Small Satellite Missions for Earth Observation*, ed. by R. Sandau, H.-P. Roeser, A. Valenzuela (Springer, Heidelberg, 2006), pp. 197–206

- Y. Takahashi, A. Yoshida, M. Sato, T. Adachi, S. Kondo, R.R. Hsu, H.T. Su, A.B. Chen, S.B. Mende, H.U. Frey, L.C. Lee, Absolute optical energy of sprites and its relationship to charge moment of parent lightning discharge based on measurement by ISUAL/AP. *J. Geophys. Res.* **115**, A00E55 (2010). doi:[10.1029/2009JA014814](https://doi.org/10.1029/2009JA014814)
- P. Tardiveau, E. Marode, A. Agneray, M. Cheaib, Pressure effects on the development of an electric discharge in non-uniform fields. *J. Phys. D, Appl. Phys.* **34**, 1690–1696 (2001)
- M. Tavani, M. Marisaldi, C. Labanti, F. Fuschino, A. Argan, A. Trois, P. Giommi, S. Colafrancesco, C. Pittori, F. Palma, M. Trifoglio, F. Gianotti, A. Bulgarelli, V. Vittorini, F. Verrecchia, L. Salotti, G. Barbiellini, P. Caraveo, P.W. Cattaneo, A. Chen, T. Contessi, E. Costa, F. D'Ammando, E. Del Monte, G. De Paris, G. Di Cocco, G. Di Persio, I. Donnarumma, Y. Evangelista, M. Feroci, A. Ferrari, M. Galli, A. Giuliani, M. Giusti, I. Lapshov, F. Lazzarotto, P. Lipari, F. Longo, S. Mereghetti, E. Morelli, E. Moretti, A. Morselli, L. Pacciani, A. Pellizzoni, F. Perotti, G. Piano, P. Picozza, M. Pilia, G. Pucella, M. Prest, M. Rapisarda, A. Rappoldi, E. Rossi, A. Rubini, S. Sabatini, E. Scalise, P. Soffitta, E. Striani, E. Vallazza, S. Vercellone, A. Zambra, D. Zanello, AGILE Team, Terrestrial Gamma-Ray Flashes as Powerful Particle Accelerators. *Phys. Rev. Lett.* **106**(1), 018501 (2011). doi:[10.1103/PhysRevLett.106.018501](https://doi.org/10.1103/PhysRevLett.106.018501)
- L.Z. Tong, K. Nanbu, H. Fukunishi, Simulation of gigantic jets propagating from the top of thunderclouds to the ionosphere. *Earth Planets Space* **57**(7), 613–617 (2005)
- E. Vadislavsky, Y. Yair, C. Erlick, C. Price, E. Greenberg, R. Yaniv, B. Ziv, N. Reicher, A. Devir, Indication for circular organization of column sprite elements associated with Eastern Mediterranean winter thunderstorms. *J. Atmos. Sol.-Terr. Phys.* **71**(17–18), 1835–1839 (2009). doi:[10.1016/j.jastp.2009.07.001](https://doi.org/10.1016/j.jastp.2009.07.001)
- O.A. van der Velde, A. Mika, S. Soula, C. Haldoupis, T. Neubert, U.S. Inan, Observations of the relationship between sprite morphology and in-cloud lightning processes. *J. Geophys. Res.* **111**, D15203 (2006). doi:[10.1029/2005JD006879](https://doi.org/10.1029/2005JD006879)
- O.A. van der Velde, W.A. Lyons, T.E. Nelson, S.A. Cummer, J. Li, J. Bunnell, Analysis of the first gigantic jet recorded over continental North America. *J. Geophys. Res.* **112**, D20104 (2007). doi:[10.1029/2007JD008575](https://doi.org/10.1029/2007JD008575)
- O.A. van der Velde, J. Bor, J. Li, S.A. Cummer, E. Arnone, F. Zanotti, M. Fullekrug, C. Haldoupis, S. NaitAmor, T. Farges, Multi-instrumental observations of a positive gigantic jet produced by a winter thunderstorm in Europe. *J. Geophys. Res.* **115**, D24301 (2010a)
- O.A. van der Velde, J. Montanya, S. Soula, N. Pineda, J. Bech, Spatial and temporal evolution of horizontally extensive lightning discharges associated with sprite-producing positive cloud-to-ground flashes in northeastern Spain. *J. Geophys. Res.* **115**, A00E56 (2010b). doi:[10.1029/2009JA014773](https://doi.org/10.1029/2009JA014773)
- G. Veronis, V.P. Pasko, U.S. Inan, Characteristics of mesospheric optical emissions produced by lightning discharges. *J. Geophys. Res.* **104**(A6), 12645–12656 (2001)
- P.A. Vitello, B.M. Penetrante, J.N. Bardsley, Simulation of negative-streamer dynamics in nitrogen. *Phys. Rev. E* **49**, 5574–5598 (1994)
- E.M. Wescott, D. Sentman, D. Osborne, D. Hampton, M. Heavner, Preliminary results from the Sprites94 aircraft campaign. 2. Blue jets. *Geophys. Res. Lett.* **22**(10), 1209–1212 (1995)
- E.M. Wescott, D.D. Sentman, M.J. Heavner, D.L. Hampton, O.H. Vaughan Jr., Blue jets: their relationship to lightning and very large hailfall, and their physical mechanisms for their production. *J. Atmos. Sol.-Terr. Phys.* **60**, 713–724 (1998)
- E.M. Wescott, D. Sentman, H.C. Stenbaek-Nielsen, P. Huet, M.J. Heavner, D.R. Moudry, New evidence for the brightness and ionization of blue jets and blue starters. *J. Geophys. Res.* **106**(A10), 21549–21554 (2001). doi:[10.1029/2000JA000429](https://doi.org/10.1029/2000JA000429)
- E. Williams, Y. Yair, The microphysical and electrical properties of sprite producing thunderstorms, in *Sprites, Elves and Intense Lightning Discharges*, ed. by M. Füllekrug, E.A. Mareev, M.J. Rycroft. NATO Science Series II: Mathematics, Physics and Chemistry, vol. 225 (Springer, Heidelberg, 2006), pp. 57–83
- E.R. Williams, The tripolar structure of thunderstorms. *J. Geophys. Res.* **94**(D11), 13151–13167 (1989)
- E.R. Williams, Problems in lightning physics—the role of polarity asymmetry. *Plasma Sources Sci. Technol.* **15**(2), S91–S108 (2006). doi:[10.1088/0963-0252/15/2/S12](https://doi.org/10.1088/0963-0252/15/2/S12)
- E.R. Williams, The global electrical circuit: a review. *Atmos. Res.* **91**(2–4) Sp. Iss. SI, 140–152 (2009). doi:[10.1016/j.atmosres.2008.05.018](https://doi.org/10.1016/j.atmosres.2008.05.018)
- C.T.R. Wilson, The electric field of a thundercloud and some of its effects. *Proc. Phys. Soc. London* **37**, 32D–37D (1925)
- Y. Yair, Observations of transient luminous events from earth orbit. *IEEE Trans. Fundam. Mater.* **126**, 244–249 (2006)
- Y. Yair, C. Price, Z. Levin, J. Joseph, P. Israelevitch, A. Devir, M. Moalem, B. Ziv, M. Asfur, Sprite observations from the space shuttle during the Mediterranean Israeli dust experiment (MEIDEX). *J. Atmos. Sol.-Terr. Phys.* **65**(5), 635–642 (2003). doi:[10.1016/S1364-6826\(02\)00332-2](https://doi.org/10.1016/S1364-6826(02)00332-2)

- Y. Yair, P. Israelevich, A.D. Devir, M. Moalem, C. Price, J.H. Joseph, Z. Levin, B. Ziv, A. Sternlieb, A. Teller, New observations of sprites from the space shuttle. *J. Geophys. Res.* **109**, D15201 (2004). doi:[10.1029/2003JD004497](https://doi.org/10.1029/2003JD004497)
- Y. Yair, C. Price, M. Ganot, E. Greenberg, R. Yaniv, B. Ziv, Y. Sherez, A. Devir, J. Bor, G. Satori, Optical observations of transient luminous events associated with winter thunderstorms near the coast of Israel. *Atmos. Res.* **91**(2–4) Sp. Iss. SI, 529–537 (2009). doi:[10.1016/j.atmosres.2008.06.018](https://doi.org/10.1016/j.atmosres.2008.06.018)
- S.A. Yashunin, E.A. Mareev, V.A. Rakov, Are lightning M components capable of initiating sprites and sprite halos?. *J. Geophys. Res.* **112**(D10), D10109 (2007)
- N.A. Zabotin, J.W. Wright, Role of meteoric dust in sprite formation. *Geophys. Res. Lett.* **28**(13), 2593–2596 (2001). doi:[10.1029/2000GL012699](https://doi.org/10.1029/2000GL012699)